# A THEORETICAL STUDY OF THE INTERACTION OF AN EDGE DISLOCATION WITH A COATED CRYSTAL BOUNDARY

Thesis for the Degree of Ph. D.
MICHIGAN STATE UNIVERSITY

Gary Hamilton Conners

1962

This is to certify that the

thesis entitled

A THEORETICAL STUDY OF THE
INTERACTION OF AN EDGE DISLOCATION
WITH A COATED CRYSTAL BOUNDARY

presented by

Gary H. Conners

has been accepted towards fulfillment
of the requirements for

Ph.D. degree in Applied Mechanics

T. Tsuffet

Major professor

Date 16 January 1963

O-169

## ABSTRACT

# A THEORETICAL STUDY OF THE INTERACTION OF AN EDGE DISLOCATION WITH A COATED CRYSTAL BOUNDARY

by Gary Hamilton Conners

Numerous experimental results have indicated that a surface layer can act as a barrier to the egress of edge dislocations from the interior of a crystal. In the present investigation, a mathematical model for this barrier effect is developed using complex variable methods of continuum elasticity theory.

A solution of the elasticity problem is first found for the case of an edge dislocation in a homogeneous half plane by employing an image dislocation. An approximate solution for the case of a half plane coated with a uniform layer of material having a different Young's modulus is then obtained by modifying this image through the introduction of a magnification factor.

This solution is employed to determine curves of force per unit length of dislocation line as a function of distance from the interface for various ratios of Young's moduli in surface layer and substrate material. In all cases this force is attractive toward the interface at a sufficiently great depth. For ratios of Young's moduli above a certain value, however, the curves pass through an equilibrium position at which the force vanishes and take on increasingrepulsive values as the interface is approached. The theory thus predicts the existence of a barrier effect, and provides an expression for the shape of the potential barrier.

# A THEORETICAL STUDY OF THE INTERACTION OF AN EDGE DISLOCATION WITH A COATED CRYSTAL BOUNDARY

By

Gary Hamilton Conners

A THESIS

Submitted to
Michigan State University
in partial fulfillment of the requirements
for the degree of

DOCTOR OF PHILOSOPHY

Department of Metallurgy, Mechanics
and Materials Science

1962

## ACKNOWLEDGMENTS

I wish to express my sincere thanks to my thesis adviser Dr. T. Triffet for acquainting me with the problem and for his excellent advice and encouragement during its investigation. I am also grateful to the other members of my committee for their interest.

Thanks are also due to my wife Gwenyth for her patience and help in preparing the manuscript, to Mr. Charles Newman for his valuable assistance with the numerical calculations, and to Delco Appliance Division of General Motors for providing for my support during the course of this work.

**********

TABLE OF CONTENTS

## LIST OF TABLES

## LIST OF FIGURES

LIST OF FIGURES - Continued

## LIST OF SYMBOLS

| | |
|---|---|
| $\lambda$ | Distance of dislocation from surface |
| $\sigma_{xx}$, $\sigma_{yy}$ | Normal stress components |
| $\sigma_{xy}$ | Shear stress |
| u, v | Displacement components |
| $\phi$, $\psi$ | Complex stress functions |
| $\Phi$, $\Psi$ | Complex stress functions, $\Phi = \phi'$, $\Psi = \psi'$ |
| $\lambda$, $\mu$ | Lamé elastic constants |
| E | Young's modulus |
| $\nu$ | Poisson's ratio |
| $\vec{b}$ | Burgers vector |
| $B_x$, $B_y$ | Burgers vector components |
| $r_0$ | Dislocation core radius |
| z | complex variable, $z \doteq x + iy$ |
| t | Position variable on real axis |
| s | Position variable on substrate--surface coating interface |
| $R_0$ | Substrate region |
| $R_1$ | Surface coating region |
| h | Coating thickness |
| $\ell$ | Distance of dislocation from interface |
| F | Force per unit length on dislocation line |
| $\sigma_{xx}^*$, $\sigma_{yy}^*$, $\sigma_{xy}^*$ | Dimensionless stresses |

# CHAPTER 1

# INTRODUCTION

## 1.1 Preliminary Remarks

It is generally accepted that dislocations play a crucial role in the deformation characteristics of crystalline solids. It follows, therefore, that any factor which significantly affects the behavior of dislocations may also be of importance in determining these characteristics for a particular solid.

The property of dislocations which will be of interest here is the stress field around them; only edge dislocations, which may be treated as producing a state of plane strain, will be considered. Since the stress components for an edge dislocation vary approximately as $1/r$ for large $r$, where $r$ is the distance from the dislocation line (1), the stress field may be said to be a long range field (see Appendix for stress field plots). This being the case, it is clear that interactions with the surface may be of importance even for dislocations well in the interior of a crystal.

As a first step, therefore, it is reasonable to attempt to determine the stress field around an edge dislocation as a function of its distance from an idealized plane boundary, assuming in particular that the elastic properties of the material do not change up to the boundary. Such a model for a boundary is certainly a very unrealistic one, however, for it is well-known that the properties at the surface of real materials may be vastly different from those in the interior. Oxide layers, adsorbed gas films, layers work hardened by machining, and various other factors serve to modify the properties of surface regions.

A better model is, therefore, one for which a layer of material with constant thickness and elastic constants different from those of the bulk material is superimposed on the plane boundary of the simple model. Such a picture is still only an approximation, since the properties of actual surface layers may vary continuously through their thickness. The introduction of the inhomogeneity into the model as represented by the idealized surface layer, however, greatly increases the probability of predicting any interesting effects which real surface layers may produce. Furthermore, for dislocations at some distance from the boundary a complicated variation in elastic properties may produce about the same overall effects as an equivalent stepwise variation.

## 1.2 Experimental Background

Before undertaking a theoretical study of the models mentioned in the preceding section, it is important to note that ample experimental evidence exists to indicate that surface conditions can, indeed, affect the overall mechanical behavior of crystalline solids. The magnitude of the observed effects is much larger than can be accounted for by the methods of classical continuum mechanics as employed, for example, in strength of materials. It therefore seems reasonable to hypothesize that the effects are caused by the interaction of the surface with the dislocation stress field; the analysis of the theoretical models is for this reason a matter of definite practical importance.

The experimental investigations to be discussed below seem to be of particular interest. In 1936, Roscoe reported that the presence of an oxide film less than twenty atoms in thickness on cadmium increased the critical shear stress by fifty per cent for a single crystal wire of 1/4 millimeter radius (2). Some of Roscoe's results are tabulated below. The quantity $S_0$ in this table is the critical shear stress.

Table I. Experimental Results of Roscoe

| Oxide Thickness | $S_0$ |
|---|---|
| 0 | 50 gm/mm$^2$ |
| 20 atoms | 75 |
| 400 atoms | 84 |
| 1200 atoms | 122 |

The thickness of the oxide layer was estimated by comparing its color with that of standard samples.

Roscoe found that his results were not dependent on the impurity content of his samples over a wide range of purities, but did depend somewhat on their crystallographic orientation. In addition he found that even at large strains where the film was apparently completely destroyed and incapable of supporting any stress itself, the stresses remained at much higher levels than those observed with unoxidized samples. This led him to the opinion that "the crystal is affected by the oxide to some considerable depth below its surface," an opinion which lends support to the assumption of a dislocation mechanism.

Following Roscoe's early work, numerous investigations of the so-called Roscoe effect have been carried out. They constitute the first class of experiments which are of interest here. The results of Andrade and his co-workers in the period around 1950 provide some of the best examples.

In 1951 Andrade and Henderson reported a marked increase in the critical shear stress of silver single crystals heated in air, from a value of about 25 gm/mm$^2$ at room temperature to about 125 gm/mm$^2$ at 500$^\circ$ C. (3). No such change was observed with crystals heated in vacuum, indicating that the increase was probably caused by the formation of an oxide layer. The layer which produced this

marked effect, however, remained too thin to be visually observed.

Also of interest is the work reported by Westwood in 1960 on the effect of surface condition on the properties of ionic crystals, in particular lithium fluoride (4). Coatings were applied to compression specimens with cross sectional areas of about 75 $mm^2$ by vacuum deposition of chromium and by chemical reaction with magnesium oxide powder. The reacted coatings were found to have the most significant effect on the mechanical properties; some of Westwood's results with these coatings are given below, the data being for two different samples:

Table II. Experimental Results of Westwood

| Coating Thickness | $S_0$ | $S_0$ |
|---|---|---|
| 0 | 120 $gm/mm^2$ | 156 $gm/mm^2$ |
| > 10 $\mu$ | 149 | --- |
| > 50 $\mu$ | --- | 256 |

The reacted layer was believed to be an alloy layer of magnesium in lithium fluoride. In addition to raising the critical shear stress, this layer markedly affected the average yield stress, average stress at fracture, average strain at fracture, and produced a "catastrophic stress drop" in the case of thin (> 10 $\mu$) films when the critical shear stress was reached.

Other important Roscoe effect experiments have been those of Mukai in 1958 which demonstrated an increase in the tensile strength of aluminum crystals which was proportional to the thickness of the oxide coating up to a thickness of 700 Å (5), of Menter and Hall in 1950 on the behavior of cadmium crystals (6) supplementing the findings of Roscoe and of Evans and Schwarzenberger in 1959 on slip processes in crystalline substrates with various coatings (7).

A second class of experiments pertinent to this study deals with the emission of acoustic pulses by deformed crystalline materials. Acoustic emissions have been extensively studied in recent years by Schofield (8), and by Tatro and his students at Michigan State University (9).

Some acoustic emissions, in particular those associated with twinning deformations as in the case of the well-known "tin cry" phenomenon, have well-established origins (8). Of greater interest are the much lower energy pulses observed during the deformation of single crystals and polycrystalline samples of various metals, including aluminum and zinc, which can not be traced to known sources.

Typical results of Schofield for an aluminum single crystal in tension show some emissions beginning at very low stresses, with the maximum emission rate of about 4,000 counts per second being attained slightly below the yield value. These emissions are of very small amplitude, requiring amplification of $10^6$ to $10^7$ times for detection and study (8).

Very recent experiments by Tatro and Liptai indicate that surface treatments, such as sand blasting or polishing, can alter markedly the emission characteristics of an aluminum specimen (10). These results demonstrate a strong dependence of acoustic emission behavior on surface properties.

## 1.3 Analysis of Experiments

While very little has been done in a quantitative way to explain the phenomena described in the preceding section, a qualitative explanation has been developed which seems adequate to explain at least the principal features of the Roscoe effect. This theory has been extended here to provide a possible explanation of acoustic emission effects as well. It must be remembered, however, that coupled with the effects on critical stress observed in the Roscoe effect are alterations in many of the other

significant mechanical properties. The complete picture for any one material is very complex, and it is unlikely that any one mechanism could be proposed which would account for all the effects in every type of material. Bearing this in mind, we can proceed to the discussion of the process which has been suggested as the dominant mechanism in the Roscoe effect.

As stated by Westwood, the central idea in this theory is that "a surface coating can act as a stable barrier to dislocations, causing pile-up, coalescence, and the formation of crack nuclei beneath the film" (4). This hypothesis was verified by his experiments with lithium fluoride, and he concluded on the basis of metallographic evidence that "surface coatings can act as barriers to the egress of edge dislocations" (4).

The suggested explanation of a surface layer's ability to function as a dislocation barrier involves consideration of the elastic strain energy stored in the crystal system. For the purposes of this discussion, a system composed of a single dislocation located a distance $\lambda$ from the plane boundary of a semi-infinite, homogenous, isotropic medium coated with a layer of material with different elastic constants will be considered. The slip plane in which the dislocation line is located will be allowed to have an arbitrary orientation with respect to the boundary.

Since the stress field in such a system will depend upon the distance $\lambda$, clearly the elastic strain energy stored in the dislocation field, which we will call $V_D$, will also be a function of $\lambda$. Then if a value $\lambda_0$ exists such that

$$\left( \frac{\partial V_D}{\partial \lambda} \right)_{\lambda=\lambda_0} = 0$$

and if this extremum corresponds to a minimum in the strain energy, $\lambda_0$ will correspond to an equilibrium position for the dislocation, i.e., a dislocation at $\lambda_0$ will lie in a potential well.

The functional dependence of $V_D$ on $\lambda$ will obviously be related to the elastic constants of the substrate and surface. Hence the possibility of the existence of a potential well will also depend upon these constants. Head investigated this possibility for a screw dislocation and found that for constants such as those for aluminum with an aluminum oxide layer, a potential minimum did exist for $\lambda$ approximately equal to h, where h is the thickness of the layer (11). He also suggested that on the basis of physical considerations such a minimum could be expected for an edge dislocation.

In order to complete the picture, the effect of applying an external stress field to the system must be considered. In such a case, the total elastic strain energy will have the form

$$V = V_D + V_E + V_I$$

where $V_E$ is the contribution from the external field, and $V_I$ is the energy of interaction of the dislocation and applied fields. The position of the energy minimum, if it exists, will then be a function of the applied stresses as well as the other variables previously mentioned; for example, one might expect that by increasing the applied stress, the equilibrium position for a dislocation trapped near a boundary would be forced closer to the boundary.

When the portion of the strain energy stored in the surface region reaches some critical value $V_C$, it might be expected that the nature of the boundary conditions at the interface between the substrate and the surface layer would be altered. Implicit in the preceding discussion has been the assumption that the layer was bonded to the substrate, i.e., attached so that the traction and displacements were continuous across the boundary. (Traction is defined as the normal and shear stresses acting on a surface.) Clearly two types of post-critical behavior can

occur in which both layer and substrate deformations remain elastic; either the layer may completely separate from the substrate over an area near the dislocation, thus ceasing to play any role in the stress picture, or it may begin to slide on the substrate, in which case only the displacement component normal to the interface must be continuous.

Either of these types of transitions will cause an immediate reduction in the strain energy, and most probably an altered dependence of V on $\lambda$ in which no minimum may exist. In order for energy to be conserved, then, the stored strain energy must be converted to other energy forms.

Part of this energy will be dissipated by frictional forces acting on the dislocation as it moves out to the surface. Another portion may go into surface energy necessary to create new surface areas. The remainder of the energy could be converted into an elastic wave which will be propagated through the crystal; this wave may be detected as an acoustic emission.

This completes the qualitative model for the observed surface effects. To summarize, the presence of a surface layer causes a dislocation to be trapped in a potential well below the surface, thus inhibiting macroscopic slip. When the applied stresses reach some critical value the strain energy is reduced due to a change in conditions at the boundary, and the dislocation is released from the barrier. The elastic strain energy stored in the dislocation field is partially converted into an elastic wave which propagates through the crystal, and is detected as an acoustic emission.

## 1.4 Objectives

The initial difficulty which must be overcome in attempting to extend the qualitative picture discussed in the preceding section to a

quantitative model which can be compared with experimental results is that of determining the stress field around a dislocation near a boundary, with various boundary conditions. Once this problem has been solved, the behavior of the dislocation can be determined for various appropriate values of the parameters involved.

The primary goal of this investigation is to solve the stress boundary value problems for the case of a free boundary and a boundary with a bonded layer. These problems will be formulated for a dislocation with arbitrary orientation, but specific solutions will be sought only in the case of the Burgers vector normal to the boundary. The complex variable methods developed for plane, small strain elasticity problems by Muskhelishvili and the Russian school of elasticians will be employed (12).

The results will then be used to obtain some quantitative estimates of the behavior of dislocations for certain particular cases; conditions under which a barrier effect can exist and the nature of the barrier will be investigated. Clearly this program constitutes only a first step toward a complete quantitative picture of such a complex phenomenon as acoustic emission. It is hoped that the results will lead to some understanding of the barrier effect, however, and will provide a foundation for further theoretical and experimental investigations.

# CHAPTER 2

# THEORETICAL BACKGROUND

## 2.1 Complex Variable Formulation of Plane Elasticity Theory

It is well-known that in plane elasticity problems, the stress components $\sigma_{xx}$, $\sigma_{yy}$ and $\sigma_{xy}$ can be obtained from a single function, the Airy stress function (13). If the stress function is represented by U, the formulas for the stresses are:

$$\sigma_{xx} = \frac{\partial^2 U}{\partial y^2} ; \quad \sigma_{yy} = \frac{\partial^2 U}{\partial x^2} ; \quad \sigma_{xy} = - \frac{\partial^2 U}{\partial x \partial y} \tag{2.1}$$

The function U must be a biharmonic function, that is, it must be a solution of the biharmonic equation

$$\nabla^4 U = \frac{\partial^4 U}{\partial x^4} + 2 \frac{\partial^4 U}{\partial x^2 \partial y^2} + \frac{\partial^4 U}{\partial y^4} = 0 \tag{2.2}$$

in order that the stresses will satisfy the conditions of compatibility.

It has been shown by Muskhelishvili that every biharmonic function U(x, y) may be represented by two functions of the complex variable $z = x + iy$ (12). Denoting these functions by $\phi(z)$ and $X(z)$, this representation is

$$2U = \bar{z}\, \phi(z) + z\, \overline{\phi(z)} + X(z) + \overline{X(z)} \tag{2.3}$$

where the bar notation (e.g., $\bar{z}$) indicates complex conjugation. Muskhelishvili further demonstrated that both of the functions $\phi(z)$ and $X(z)$ must be holomorphic, that is, single-valued and analytic, in any simply connected region.

By differentiation the following expressions for $\frac{\partial U}{\partial x}$ and $\frac{\partial U}{\partial y}$ are found:

$$2\frac{\partial U}{\partial x} = \phi(z) + \bar{z}\,\phi'(z) + \overline{\phi(z)} + z\overline{\phi'(z)} + X'(z) + \overline{X'(z)}$$

$$2\frac{\partial U}{\partial y} = i[-\phi(z) + \bar{z}\,\phi'(z) + \overline{\phi(z)} - z\overline{\phi'(z)} + X'(z) - \overline{X'(z)}] \qquad (2.4)$$

These results can then be combined to give a simple expression for $\frac{\partial U}{\partial x} + i\frac{\partial U}{\partial y}$ ;

$$\frac{\partial U}{\partial x} + i\frac{\partial U}{\partial y} = \phi(z) + z\overline{\phi'(z)} + \Psi(z) \qquad (2.5)$$

where $\Psi(z) = \frac{dX}{dz}$ .

Formulas for the stresses in terms of the holomorphic functions $\Psi(z)$ and $\phi(z)$ can be obtained by considering the force acting on an element of arc ds in the x, y plane with unit normal vector $\hat{n}$ and unit tangent vector $\hat{t}$, as shown in Figure 1.

If the force acting on ds has components ($\sigma_{xn}$ ds, $\sigma_{yn}$ ds) these will be related to the stresses by:

$$\sigma_{xn} = \sigma_{xx}\cos(n,x) + \sigma_{xy}\cos(n,y) = \frac{\partial^2 U}{\partial y^2}\cos(n,x) - \frac{\partial^2 U}{\partial x \partial y}\cos(n,y)$$

$$\sigma_{yn} = \sigma_{yx}\cos(n,x) + \sigma_{yy}\cos(n,y) = -\frac{\partial^2 U}{\partial x\,\partial y}\cos(n,x) + \frac{\partial^2 U}{\partial x^2}\cdot\cos(n,y) \qquad (2.6)$$

Note that $\sigma_{xy} = \sigma_{yx}$ because of the symmetry of the stress tensor.
Now cos (n, x) = dy/ds and cos (n, y) = -dx/ds.
Hence,

$$\sigma_{xn} = \frac{d}{ds}\left(\frac{\partial U}{\partial y}\right) ; \quad \sigma_{yn} = -\frac{d}{ds}\left(\frac{\partial U}{\partial x}\right)$$

In complex form,

$$(\sigma_{xn} + i\,\sigma_{yn})ds = -\,id\left(\frac{\partial U}{\partial x} + i\frac{\partial U}{\partial y}\right) \qquad (2.7)$$

or, by means of equation (2.5),

$$(\sigma_{xn} + i\,\sigma_{yn})ds = -\,i\,d\,[\phi(z) + z\,\overline{\phi'(z)} + \overline{\Psi(z)}] \qquad (2.8)$$

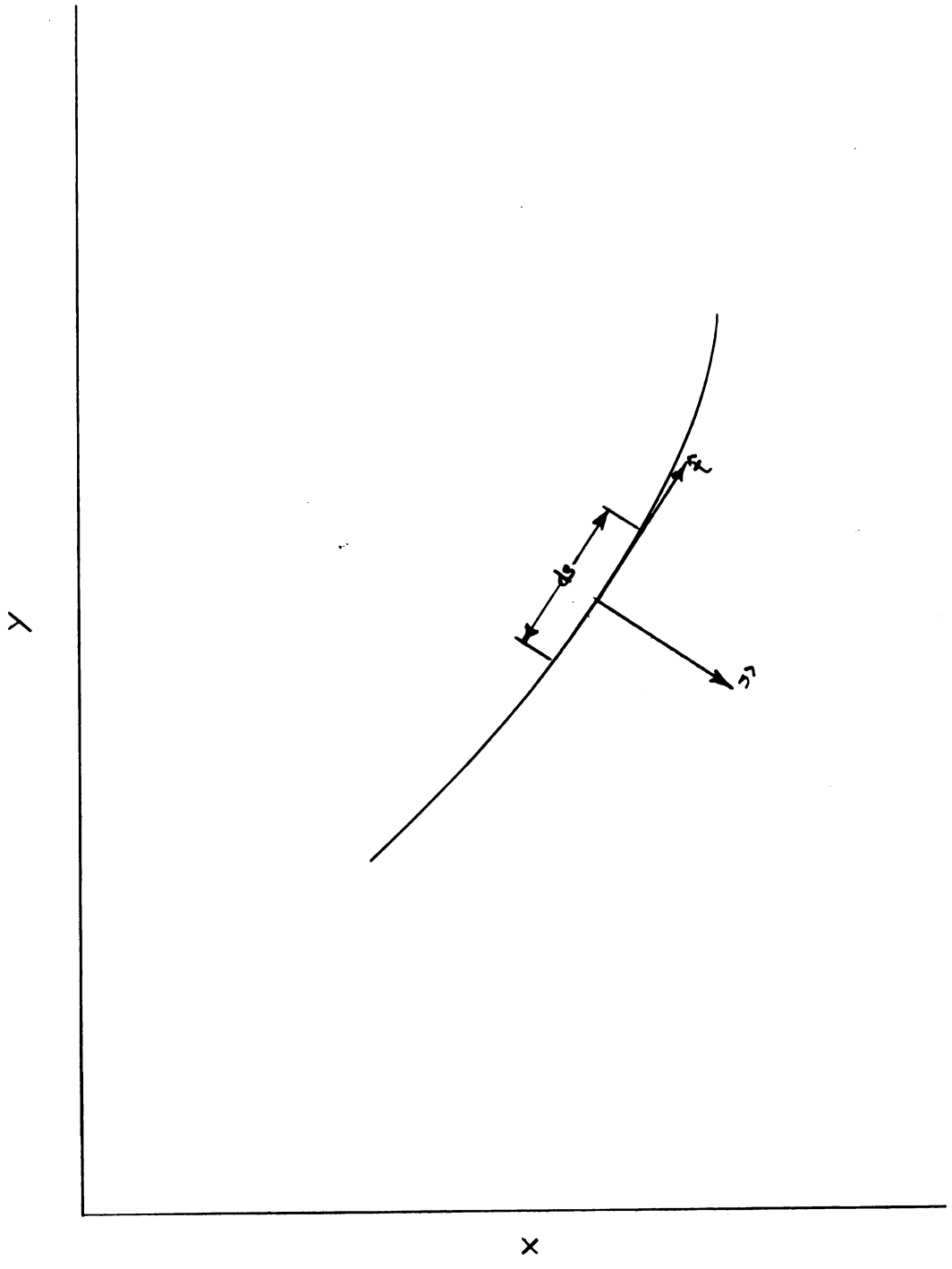


Figure 1. Arc geometry used in deriving stress formulas.

Letting $\hat{n}$ be in the direction of the x- axis,

$$\sigma_{xx} + i\,\sigma_{xy} = \phi'(z) + \overline{\phi'(z)} - z\overline{\phi''(z)} - \overline{\psi'(z)} \tag{2.9}$$

Similarly, by letting $\hat{n}$ be in the direction of the y- axis,

$$\sigma_{yy} - i\,\sigma_{xy} = \phi'(z) + \overline{\phi'(z)} + z\overline{\phi''(z)} + \overline{\psi'(z)} \tag{2.10}$$

The most useful representations for the stresses are obtained by combining the final two results. It is also convenient to adopt the notation

$$\Phi(z) = \phi'(z) \quad \text{and} \quad \Psi(z) = \psi'(z) . \tag{2.11}$$

The following formulas are then obtained:

$$\begin{aligned} \sigma_{xx} + \sigma_{yy} &= 2\left[\Phi(z) + \overline{\Phi(z)}\right] = 4\,\mathrm{Re}\,\Phi(z) \\ \sigma_{yy} - \sigma_{xx} + 2i\,\sigma_{xy} &= 2\left[\bar{z}\,\Phi'(z) + \Psi(z)\right] \end{aligned} \tag{2.12}$$

Plane elasticity problems involving only stresses thus reduce to finding complex function $\Phi(z)$ and $\Psi(z)$ which will give stresses satisfying particular boundary conditions. These functions, therefore, are analogous to the Airy stress function in the more familiar formulation of elasticity theory. If displacements are also of interest, as, for example, in cases where displacement boundary conditions are given, the functions $\phi(z)$ and $\psi(z)$ are also needed. The formula derived by Muskhelishvili for the displacement components (u, v) has the form

$$2\mu(u + iv) = \kappa\phi(z) - z\,\overline{\phi'(z)} - \overline{\psi(z)} \tag{2.13}$$

where $\mu$ and $\kappa$ are elastic constants for a homogeneous, isotropic substance.

The constant $\mu$ has its usual significance as one of the Lamé constants. The constant $\kappa$ is related to the Lamé constants by

$$\kappa = \frac{\lambda + 3\mu}{\lambda + \mu} \tag{2.14}$$

in the case of plane strain. The Lamé constants $\lambda$ and $\mu$ may be obtained from the more common elastic constants E, Young's modulus, and $\nu$ Poisson's ratio , by the following formulas:

$$\lambda = \frac{E\nu}{(1+\nu)(1-2\nu)} \tag{2.15}$$

$$\mu = \frac{E}{2(1+\nu)} \tag{2.16}$$

Having established the basic equations of the complex formulation of elasticity theory, we can proceed to investigate methods by which this formulation can be applied to dislocation problems. It will be necessary first, however, to discuss some of the fundamental ideas of the theory of dislocations which will be of importance in the subsequent development.

## 2.2 Elastic Dislocation Theory; General Concepts

Edge dislocations of the type to be considered here may be pictured as being produced by cutting a thick-walled cylinder as shown in Figure 2 along the plane AB, displacing the upper cut surface a distance $B_x$ in the negative x direction while leaving the lower surface fixed, and then rejoining the cut surfaces (1). Clearly the displacements in the cylinder will not be single valued after this process is completed, since u slightly above the plane AB will differ from u slightly below this plane by an amount $B_x$.

Non-single-valued displacements of this type constitute one of the types of deformations first studied in detail by Volterra and termed

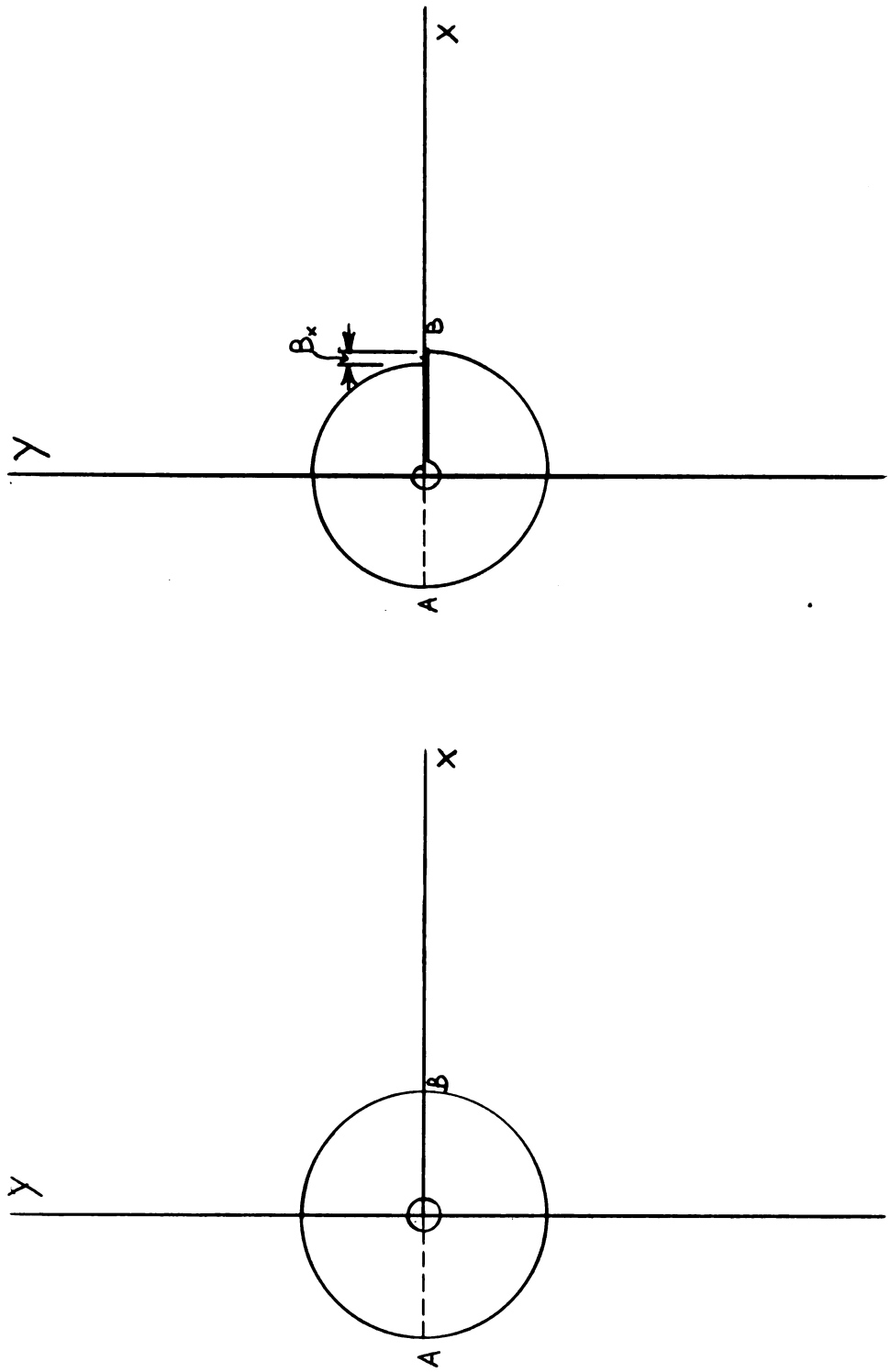


Figure 2. The formation of an edge dislocation.

dislocations by Love (14); expressions for the stresses obtained by Volterra and others, with the assumption that the material is homogeneous and isotropic, are, as given by Cottrell (1):

$$\sigma_{xx} = \frac{KB_x}{(x^2+y^2)^2}\ (-3x^2y - y^3)$$

$$\sigma_{yy} = \frac{KB_x}{(x^2+y^2)^2}\ (x^2y - y^3) \qquad (2.17)$$

$$\sigma_{xy} = \frac{KB_x}{(x^2+y^2)^2}\ (x^3 - xy^2)$$

The constant K in these formulas is given by

$$K = \frac{\mu}{2\pi\ (1-\nu)}\ . \qquad (2.18)$$

It is apparent from the discussion of the Volterra dislocation that such a dislocation could not occur in a simply connected medium. Furthermore, since the stress components as given by equations (2.17) approach infinity near the origin of coordinates, these equations could not be valid if there were material present in this region. Volterra dislocation theory can, therefore, only be applied to dislocations in crystals if it is assumed that a "core" of crystalline material has been removed along the longitudinal axis of the dislocation. The radius of this core must be sufficiently large so that the stresses and strains on its boundary will not exceed the range of validity of linear elasticity theory.

Physically the core represents the region where the concept of stress in an elastic continuum ceases to be valid, and must be replaced by detailed considerations of interparticle forces. The core radius, $r_0$, may be taken to be less than 10 $B_x$. Since core structure will not be taken into account in the applications discussed here, this distance places a lower bound on the range of applicability of the results to be obtained.

In addition, a considerable simplification in the application of dislocation theory to crystals is obtained by assuming that the crystalline material is isotropic. This assumption, which will be made here, is not a necessary one in principle, however, and some work in dislocation theory has been carried out without making it. Dislocation stress fields in anisotropic media have been studied by several investigators, notably Burgers (15) and Eshelby (16). No fundamentally different results would be expected for the problems to be considered in this study if the added complication of anisotropy were to be taken into account.

As a final consideration in the application of continuum dislocation theory to crystals, it is convenient to be able to represent the discontinuity in displacement by a vector making an arbitrary angle with the x axis, rather than restricting it to the x direction. If this vector is represented by $\vec{b}$, it may be written in terms of its components as:

$$\vec{b} = B_x \hat{i} + B_y \hat{j}$$

Since the region of interest is that where linear elasticity theory applies, $\vec{b}$ may be regarded as the result of superimposing two separate dislocations, one produced by the cutting, displacing and rejoining process discussed at the beginning of this section and the other by repeating this process with displacements in the y direction.

The vector $\vec{b}$ is referred to in crystal dislocation theory as the Burgers vector (1). It lies in the slip plane, and points in the direction of slip. Since the Burgers vector may have any direction in the (x, y) plane, the slip direction may take on any value in this range. The direction and magnitude of the Burgers vector will be determined by the crystal structure of a particular material, the slip planes and directions being in general planes and directions of highest atomic density while the magnitude will be equal to the lattice spacing in the slip direction.

Expressions for the stress components of a dislocation having both x and y components are as follows:

$$\sigma_{xx} = \frac{K}{(x^2+y^2)^2}\left[B_x(-3x^2y - y^3) + B_y(-x^3 + xy^2)\right]$$

$$\sigma_{yy} = \frac{K}{(x^2+y^2)^2}\left[B_x(x^2y - y^3) + B_y(-x^3 - 3xy^2)\right] \qquad (2.19)$$

$$\sigma_{xy} = \frac{K}{(x^2+y^2)^2}\left[B_x(x^3 - xy^2) + B_y(-x^2y + y^3)\right]$$

It should also be noted that the core radius must now depend on $|\bar{b}|$ rather on $B_x$ only. The value $r_0 = 10\,|\bar{b}|$ will be assumed here, unless otherwise indicated.

## 2.3 Elastic Dislocation Theory; Complex Methods

In applications of complex elasticity theory to regions which are not simply connected, as in the case of a half plane with a dislocation core removed, the functions $\Phi(z)$ and $\Psi(z)$ may be such that they have singularities in the core region. Further, it is found by Muskhelishvili that if these functions are to correspond to displacements which are not single valued and stresses which are single valued, they must have the form

$$\Phi_0(z) = \frac{a + ib}{Z} = \Psi_0(z) = \frac{c + id}{Z} \qquad (2.20)$$

where a, b, c and d are real constants. By using the stress formulas (2.11) and (2.12) the following expressions for the stress components are readily obtained:

$$\sigma_{xx} = \frac{1}{(x^2+y^2)^2}\left[(3a - c)\,x^3 + (5b - d)\,x^2y + (-a-c)xy^2 + (b-d)y^3\right] \qquad (2.21)$$

$$\sigma_{yy} = \frac{1}{(x^2+y^2)^2}\left[(a+c)x^3 + (-b+d)x^2y + (5a + c)xy^2 + (3b + d)\,y^3\right] \qquad (2.22)$$

$$\sigma_{xy} = \frac{1}{(x^2+y^2)^2}\left[(-b+d)x^3 + (3a + c)x^2y + (3b +s)xy^2 + (-a-c)y^3\right] \quad (2.23)$$

These expressions will agree with those of Cottrell for an edge dislocation located at x = o, y = o if the constants are assigned the following values:

$$a = -\frac{KB_y}{2} \qquad b = -\frac{KB_x}{2}$$
$$c = -\frac{KB_y}{2} \qquad d = +\frac{KB_x}{2} \quad (2.24)$$

Thus the complex stress functions which describe the stress field of an edge dislocation at the origin of coordinates are as follows:

$$\Phi_0(z) = -\frac{K}{2} \cdot \frac{B_y + iB_x}{z}$$
$$\Psi_0(z) = -\frac{K}{2} \cdot \frac{B_y - iB_x}{z} \quad (2.25)$$

It is evident from equations (2.19) that the stresses given by these functions vanish at infinity; they are, therefore, satisfactory for describing the stress field of a dislocation in an infinite medium with no traction on the boundaries. In the cases of present interest where semi-infinite media will be dealt with, the functions $\Phi(z)$ and $\Psi(z)$ must be modified so that the stresses calculated from them will satisfy boundary conditions on the boundaries which are not at infinity.

This will be attempted here by assuming that

$$\Phi(z) = \Phi_0(z) + \Phi^*(z)$$

$$\Psi(z) = \Psi_0(z) + \Psi^*(z)$$

where $\Phi^*(z)$ and $\Psi^*(z)$ are functions holomorphic in the region of interest. These functions correspond to a stress field superimposed on that of the dislocation but since they are holomorphic do not represent

any new dislocation in the material. The problems to be studied here involve determining what form $\Phi^*(z)$ and $\Psi^*(z)$ must have in order to satisfy particular boundary conditions.

# CHAPTER 3

## BOUNDARY VALUE PROBLEMS

### 3.1 Homogeneous Half Plane

The first problem to be considered is that of a dislocation in a half plane for which the elastic constants do not vary up to the boundary. Figure 3 illustrates the geometry of the problem. An edge dislocation with Burgers vector $\vec{b}$ is located in the point $-i\lambda$ in the complex plane. It is assumed that the boundary $y = o$ is traction free, i.e., has no normal or shear stress acting on it.

Since the dislocation is not located at the origin in this problem, the stress functions $\Phi_0(z)$ and $\Psi_0(z)$ must be changed so that they have singularities at $z = -i\lambda$. They become

$$\Phi_0(z) = -\frac{K}{2} \cdot \frac{B_y + iB_x}{z + i\lambda}$$

$$\Psi_0(z) = -\frac{K}{2} \cdot \frac{B_y - iB_x}{z + i\lambda} \qquad (3.1)$$

We must then seek functions $\Phi^*(z)$ and $\Psi^*(z)$ having no singularities in the lower half plane, and such that when the stresses are calculated using the combined stress functions

$$\Phi(z) = \Phi_0(z) + \Phi^*(z)$$

and

$$\Psi(z) = \Psi_0(z) + \Psi^*(z)$$

they will satisfy the stress boundary conditions

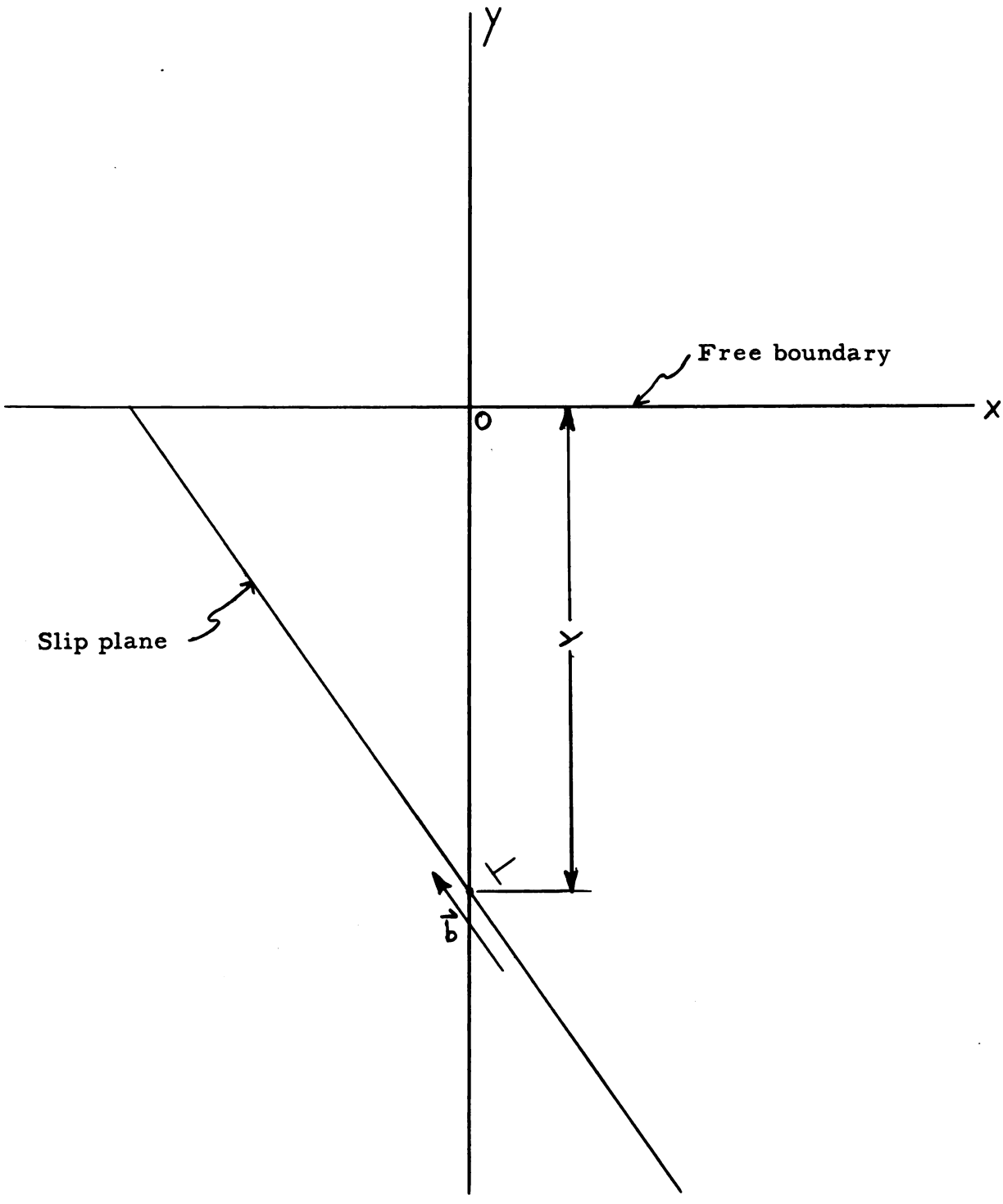


Figure 3. The geometry associated with an edge dislocation in a homogeneous half plane.

$$\left.\begin{aligned}\sigma_{yy} &= 0\\ \sigma_{xy} &= 0\end{aligned}\right\} \text{ at } y = 0 . \tag{3.2}$$

A reasonable choice to investigate for the functions desired is

$$\begin{aligned}\Phi_1^*(z) &= \frac{K}{2} \cdot \frac{\alpha + i\beta}{z - i\lambda}\\ \Psi_1^*(z) &= \frac{K}{2} \cdot \frac{\gamma + i\delta}{z - i\lambda}\end{aligned} \tag{3.3}$$

These functions represent the stress field of an arbitrary "image" dislocation located at a point conjugate to the location of the real dislocation.

Then evaluating the stresses at y = o and substituting in the boundary conditions, one obtains

$$\begin{aligned}[\sigma_{yy}]_{y=0} = \frac{K}{2(x^2+\lambda^2)^2} [&(-2B_y + \alpha + \gamma)x^3 +\\ &(2B_x + \beta - \delta)\lambda x^2 + (-6B_y + 5\alpha + \gamma)\lambda^2 x\\ &+ (-2B_x - 3\beta - \delta)\lambda^3] = 0\end{aligned} \tag{3.4}$$

$$\begin{aligned}[\sigma_{xy}]_{y=0} = \frac{K}{2(x^2+\lambda^2)^2} [&(2B_x - \beta + \delta)x^3 +\\ &(-2B_y - 3\alpha + \gamma)\lambda x^2 + (-2B_x + 3\beta + \delta)\lambda^2 x\\ &+ (2B_y + \alpha + \delta)\lambda^3] = 0\end{aligned} \tag{3.5}$$

Equations (3.4) and (3.5) will be satisfied for all values of x if and only if the coefficients of all powers of x in the terms in square brackets vanish identically. This condition provides a set of eight linear algebraic equations for the undetermined constants $\alpha$, $\beta$, $\gamma$, and $\delta$ as follows:

$$\begin{aligned} \alpha + \gamma &= 2B_y & \qquad -3\alpha + \gamma &= 2B_y \\ 5\alpha + \gamma &= 6B_y & \qquad \alpha + \gamma &= -2B_y \end{aligned} \tag{3.6}$$

$$\begin{aligned} \beta - \delta &= -2B_x & \qquad -\beta + \delta &= -2B_x \\ -3\beta - \delta &= 2B_x & \qquad 3\beta + \delta &= 2B_x \end{aligned} \tag{3.7}$$

It is readily seen that no non-trivial solution exists for this set of equations. A useful approximate solution, however, is obtained by setting

$$\begin{aligned} \alpha &= B_y & \qquad \gamma &= B_y \\ \beta &= -B_x & \qquad \delta &= B_x \end{aligned} \tag{3.8}$$

This choice of values signifies in physical terms that the Burgers vector of the image dislocation be taken as the mirror image of the Burgers vector of the real dislocation under reflection in the real axis. Such a selection for the image is equivalent to an approximate solution arrived at by Koehler (17) and others by different methods. Its effect is to satisfy the boundary conditions on the normal stress but to double the shear stress on the boundary.

This failure of the image solution to satisfy all of the boundary conditions on the problem can be remedied by superimposing an additional solution on it. One would expect this to be the case on physical grounds, since a dislocation of the type considered here can certainly exist in an elastic material, indicating that a solution to the elasticity problem exists.

It is shown by Muskelishvili (12) that in a half plane problem for a homogeneous medium only one of the usual stress functions may be considered as independent. If $\Phi_2^*(z)$ and $\Psi_2^*(z)$ are taken as the stress functions for the additional superposition field, then $\Phi_2^*(z)$ may be regarded as the independent function. Once $\Phi_2^*(z)$ is found, $\Psi_2^*(z)$ can be determined from it by means of known formulas (12).

Letting $t$ be the position variable along the real axis, the boundary conditions for the problem of determining $O_2^*(z)$ are

$$\sigma_{xy_2}^{*}(t) + 2\,\sigma_{xy}^{o}(t) = 0$$

$$\sigma_{yy_2}^{*}(t) = 0 \qquad (3.9)$$

where the superscript $0$ indicates the contribution from the dislocation field, while the $*$ terms with subscript $2$ arise from the additional superimposed stress field.

It can be shown that the solutions to this problem is given by the Cauchy integral

$$\Phi_2^*(z) = \frac{1}{2\pi i}\int_{-\infty}^{\infty} \frac{2\sigma_{xy}^{o}(t)}{t - z}\,dt \qquad (3.10)$$

Since $\sigma_{xy}^{o}(t)$ is a real function and decreases as $1/t$ for large $t$,

$\Phi_2^*(t)$ as given by (3.10) must necessarily be a holomorphic function. The existence of a solution to the problem is therefore proven.

The integral in (3.10) may readily be evaluated by the usual method of closing the contour of integration with an infinite semicircle in the lower half plane and calculating the residues at the poles inside this contour. As may be seen from equation (3.5), there are poles at $-i\lambda$ and at z, which may range over the lower half plane. In calculating $\Phi_2^*(-i\lambda)$ for example, one has a pole of order three at $-i\lambda$ so that

$$\Phi_2^*(-i\lambda) = \frac{iK}{2}\left[\frac{d^2}{dt^2}\left\{\frac{(t+i\lambda)^3}{(t^2+\lambda^2)(t+i\lambda)}\cdot 4(B_x t^3 - B_y\lambda t^2 - B_x\lambda^2 t + B_y\lambda^3)\right\}\right]_{t=-i} \tag{3.11}$$

The shear stress evaluated at $-i\lambda$ is an important factor in calculating the force on the real dislocation, as will be seen later. The contribution to this from the stress function (3.11) is found negligible by Koehler; thus for purposes of calculating this force, it is sufficient to consider only the stresses due to the image dislocation.

## 3.2 The Coated Plane Problem

It is now of interest to consider the problem of the preceding section when a layer of material of thickness h adjacent to the real axis has elastic constants different from those in the remainder of the lower half plane. These two regions will be referred to as the surface layer and the substrate; the geometry is shown in Figure 4.

For convenience the notation $R_0$ will be used to represent the substrate region, and $R_1$ will denote the surface layer which is assumed to be bonded to $R_0$. In addition, s will be employed as the position variable on the interface, i.e., on the common boundary of $R_0$ and $R_1$. The variable t will be the position variable on the real axis, as in the preceding section.

The conditions to be satisfied in this problem are that traction and displacements must be continuous across the interface, and traction must

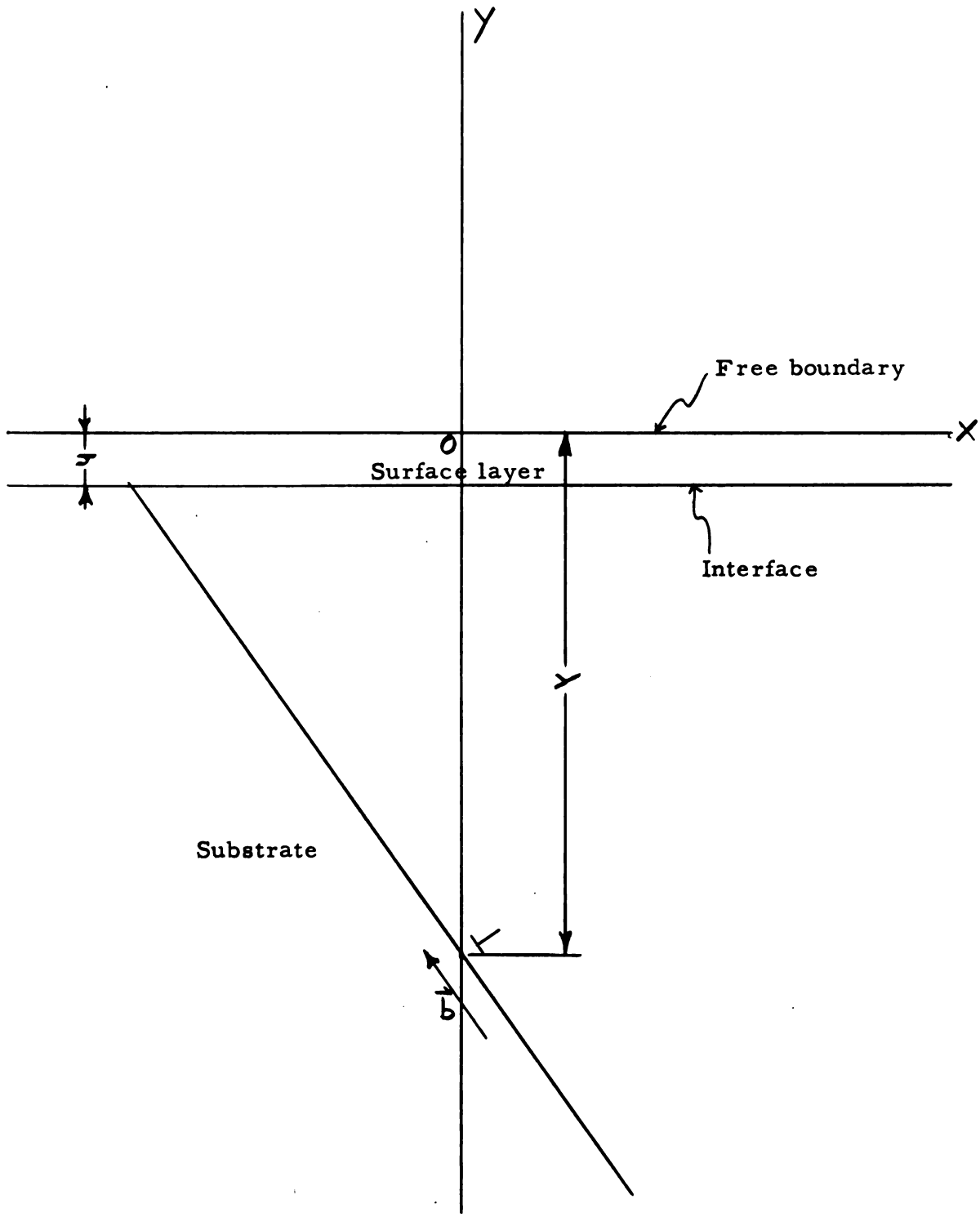


Figure 4. The geometry associated with an edge dislocation in a coated half plane.

vanish on the free boundary. These conditions must be stated in terms of the stress functions in the region $R_0$ and $R_1$. Before this can be accomplished, some additional notation is required. Stress functions for $R_0$ will be indicated by the subscript $_0$ written on the left, while those in $R_1$ will have the subscript $_1$ written in the same way. Thus $_0\Phi$ and $_0\Psi$ are the stress functions in $R_0$, and $_1\Phi$ and $_1\Psi$ are the stress functions for $R_1$.

By means of equation (2.10), the condition for continuity of the traction across the interface can be written in the form:

$$\begin{aligned} &{}_0\Phi(s) + {}_0\overline{\Phi(s)} + s\,{}_0\overline{\Phi'(s)} + {}_0\overline{\Psi(s)} = \\ &{}_1\Phi(s) + {}_1\overline{\Phi(s)} + s\,{}_1\overline{\Phi'(s)} + {}_1\overline{\Psi(s)} \end{aligned} \tag{3.12}$$

Similarly, by means of (2.13) the condition for continuity of the displacements can be written as

$$\begin{aligned} &\frac{1}{2\mu_0}\left[\kappa_0\ {}_0\phi(s) - s\,{}_0\overline{\Phi(s)} - {}_0\overline{\Psi(s)}\right] = \\ &\frac{1}{2\mu_1}\left[\kappa_1\ {}_1\phi(s) - s\,{}_1\overline{\Phi(s)} - {}_1\overline{\Psi(s)}\right] \end{aligned} \tag{3.13}$$

where the subscripts on the constants indicate the region in which they are appropriate.

A more useful equation is obtained by differentiation of (3.13), which yields

$$\begin{aligned} &\frac{1}{2\mu_0}\left[\kappa_0\ {}_0\Phi(s) - {}_0\overline{\Phi(s)} - s\,{}_0\overline{\Phi'(s)} - {}_0\overline{\Psi(s)}\right] = \\ &\frac{1}{2\mu_1}\left[\kappa_1\ {}_1\Phi(s) - {}_1\overline{\Phi(s)} - s\,{}_1\overline{\Phi'(s)} - {}_1\overline{\Psi(s)}\right] \end{aligned} \tag{3.14}$$

Equations (3.12) and (3.14) can then be combined to obtain

$$ {}_1\Phi(s) = \frac{\mu_0 + \mu_1 \kappa_0}{\mu_0 (1 + \kappa_1)} \; {}_0\Phi(s) + $$

$$ \frac{\mu_0 - \mu_1}{\mu_0(1 + \kappa_1)} \; [\, {}_0\overline{\Phi(s)} + s \, {}_0\overline{\Phi'(s)} + {}_0\overline{\Psi(s)} \,] \qquad (3.15) $$

It is now convenient to let

$$ K_1 = \frac{\mu_0 + \mu_1 \kappa_0}{\mu_0 (1 + \kappa_1)} $$

and

$$ K_2 = \frac{\mu_0 - \mu_1}{\mu_0(1 + \kappa_1)} $$

Then one has

$$ {}_1\Phi(s) = K_1 \, {}_0\Phi(s) + K_2 \, [\, {}_0\overline{\Phi(S)} + s \, {}_0\overline{\Phi'(s)} + {}_0\overline{\Psi(s)} \,] \qquad (3.16) $$

Equation (3.16) can then be combined with 3.12) to determine an expression for ${}_1\overline{\Psi(s)}$. It is found to be:

$$ {}_1\overline{\Psi(s)} = {}_0\overline{\Psi(s)} + (1 - K_1) \, [\, {}_0\Phi(s) + {}_0\overline{\Phi(s)} + s \, {}_0\Phi'(s) \,] $$

$$ - K_2 \, [2\mathrm{Re} \; {}_0\Phi(s) + {}_0\overline{\Psi(s)} + s \, {}_0\overline{\Phi'(s)} + s \frac{d}{ds} \{ \, {}_0\Phi(s) + \qquad (3.17) $$

$$ \overline{s} \, {}_0\Phi'(s) + {}_0\Psi(s) \, ] $$

Before continuing the analysis, it is useful to express the constants $K_1$ and $K_2$ in terms of familiar quantities, by means of equations (2.14) through (2.16). These constants have a particularly simple form in the case when Poisson's ratio $\nu$ has the same value in both $R_0$ and $R_1$. In this case, which will be closely approximated in most physical circumstances,

$$ K_1 = \frac{E_0 + E_1 (3 - 4\nu)}{4E_0 (1 - \nu)} $$

$$ K_2 = \frac{E_0 - E_1}{4E_0 (1 - \nu)} \qquad (3.18) $$

where $E_0$ and $E_1$ are Young's moduli in $R_0$ and $R_1$ respectively. For convenience in making numerical calculations we will assume $\nu = \frac{1}{4}$; then

$$K_1 = \frac{1}{3}\left(1 + 2\,\frac{E_1}{E_0}\right)$$
$$K_2 = \frac{1}{3}\left(1 - \frac{E_1}{E_0}\right) \tag{3.19}$$

Letting $\frac{E_1}{E_0} = 1 + 3\epsilon$, we have

$$K_1 = 1 + 2\epsilon$$
$$K_2 = -\epsilon \tag{3.20}$$

We may then write from equations (3.16) and (3.17)

$${}_1\bar{\Phi}(s) = {}_0\bar{\Phi}(s) + \epsilon F(s)$$
$${}_1\bar{\Psi}(s) = {}_0\bar{\Psi}(s) + \epsilon G(s) \tag{3.21}$$

where $F(s)$ and $G(s)$ are given by

$$F(s) = 2\,{}_0\bar{\Phi}(s) - {}_0\overline{\bar{\Phi}(s)} - s\,{}_0\overline{\bar{\Phi}'(s)} - {}_0\overline{\bar{\Psi}(s)}$$
$$G(s) = -2\mathrm{Re}\left\{{}_0\bar{\Phi}(s) - {}_0\bar{\Psi}(s)\right\} + 2\mathrm{I_m}\left\{s\,{}_0\overline{\bar{\Phi}'(s)}\right\} + s\frac{d}{ds}\left\{{}_0\bar{\Phi}(s) + s\,{}_0\overline{\bar{\Phi}'(s)} + {}_0\overline{\bar{\Psi}(s)}\right\} \tag{3.22}$$

Equations (3.21) express the continuity conditions in terms of the parameter $\epsilon$, which is a measure of the discontinuity in the material properties. Clearly in the case $\epsilon = 0$, that is, when the surface layer has the same elastic constants as the substrate, these conditions reduce simply to

$$
\begin{aligned}
{}_1\Phi(s) &= {}_0\Phi(s) \\
{}_1\Psi(s) &= {}_1\Psi(s)
\end{aligned}
\tag{3.23}
$$

The problem which must now be solved is to determine ${}_1\Phi(z)$ and ${}_1\Psi(z)$ such that the condition that the free boundary must be traction free will be satisfied, in addition to satisfying the continuity conditions (3.21). By means of equation (2.10), the condition at the free boundary may be expressed in the form

$$
{}_1\Phi(t) + \overline{{}_1\Phi(t)} + t\,\overline{{}_1\Phi'(t)} + \overline{{}_1\Psi(t)} = 0 \tag{3.24}
$$

Equations (3.21) and (3.24), along with the usual conditions that all functions vanish as $|z|$ approaches $\infty$, constitute the complete statement of the boundary conditions on the problem. One would expect, however, that although a solution probably exists which will satisfy these conditions completely, such a solution would probably be too unwieldy for practical applications. The procedure which will be followed in solving the coated plane problem will, therefore, be to weaken the boundary conditions by retaining only their real parts when the complete conditions lead to excessive complications. By analogy with the preceding problem, such a procedure may be expected to provide a good approximation for the stresses in the neighborhood of the dislocation.

# CHAPTER 4

## COATED PLANE SOLUTION AND APPLICATIONS

### 4.1 Solution

We begin by rewriting the first of equations (3.21) in the form

$$ {}_1\bar{\Phi}(s) = K_1\, {}_0\bar{\Phi}(s) - \epsilon F_1(s) \tag{4.1} $$

where

$$ F_1(s) = -F(s) + 2_0\bar{\Phi}(s) \tag{4.2} $$

The conditions at the interface may then be expressed in their weakened form as

$$ \begin{aligned} {}_1\bar{\Phi}(s) &= K_1\, {}_0\bar{\Phi}(s) - \epsilon\, p_1(s) \\ {}_1\bar{\Psi}(s) &= {}_0\bar{\Psi}(s) + \epsilon\, p_2(s) \end{aligned} \tag{4.3} $$

where

$$ \begin{aligned} p_1(s) &= \mathrm{Re}\, F_1(s) \\ p_2(s) &= \mathrm{Re}\, G(s) \end{aligned} \tag{4.4} $$

Equations (4.3) will be satisfied if in the region $R_1$ the functions ${}_1\bar{\Phi}(z)$ and ${}_1\bar{\Psi}(z)$ are as follows:

$$ \begin{aligned} {}_1\bar{\Phi}(z) &= K_1\, {}_0\bar{\Phi}(z) - \epsilon\, P_1(z) \\ {}_1\bar{\Psi}(z) &= {}_0\bar{\Psi}(z) + \epsilon\, P_2(z) \end{aligned} \tag{4.5} $$

In these equations, $P_1(z)$ and $P_2(z)$ are functions whose real parts have the boundary values $p_1(s)$ and $p_2(s)$ respectively on the interface. These functions may readily be constructed by means of a power series expansion; such a construction will clearly be a useful one here since h, the thickness of the surface layer, is almost always very small in cases of physical interest, so that only the first few terms in the expansion will need to be retained.

Writing s explicitly as (x-ih), the series representations are as follows:

$$P_1(x, y) = p_1(x-ih) + i(h+y)\cdot \frac{\partial p_1(x-ih)}{\partial x} - \frac{(h+y)^2}{2}\cdot \frac{\partial^2 p_1(x-ih)}{\partial x^2} - i\,\frac{(h+y)^3}{6}\cdot \frac{\partial^3 p_1(x-ih)}{\partial x^3} + \text{----} \tag{4.6}$$

and

$$P_2(x, y) = p_2(x-ih) + i(h+y)\cdot \frac{\partial p_2(x-ih)}{\partial x} - \frac{(h+y)^2}{2}\cdot \frac{\partial^2 p_2(x-ih)}{\partial x^2} - i\,\frac{(h+y)^3}{6}\cdot \frac{\partial^3 p_2(x-ih)}{\partial x^3} + \text{---} \tag{4.7}$$

It can be shown by applying the Cauchy-Riemann conditions that functions obtained in this manner are analytic.

An important goal has now been reached. The functions ${}_1\Phi(z)$ and ${}_1\Psi(z)$ can be completely determined by means of (4.5), (4.6), and (4.7) in region $R_1$ if ${}_0\Phi(z)$ and ${}_0\Psi(z)$ are prescribed in $R_0$; that is, for a particular stress distribution in the substrate, the distribution in the surface layer can be calculated. The problem is then to find ${}_0\Phi(z)$ and ${}_0\Psi(z)$ such that the stress on the free boundary will satisfy condition (3.24), or a weakened form of this condition.

As in the case of the homogeneous half plane, one has

$$\begin{aligned} {}_0\Phi(z) &= {}_0\Phi_0(z) + {}_0\Phi^*(z) \\ {}_0\Psi(z) &= {}_0\Psi_0(z) + {}_0\Psi^*(z) \end{aligned} \tag{4.8}$$

where ${}_0\Phi_0(z)$ and ${}_0\Psi_0(z)$ are the stress functions representing the dislocation stress field as given by equations (3.1), and ${}_0\Phi^*(z)$ and ${}_0\Psi^*(z)$ represent the superposition field. Also as in that problem, the superposition field will be obtained by an image method. The classical method of attacking a problem of this type involving two plane boundaries is to use an infinite series of images, the location of each being determined by analogy with the corresponding optical problem. We will proceed in a somewhat different manner, however, and seek a solution by means of a single image described by the following functions:

$$
\begin{aligned}
{}_0\Phi^*(z) &= \frac{K}{2} \cdot \frac{NB_y - i\,MB_x}{z - i\lambda} \\
{}_0\Psi^*(z) &= \frac{K}{2} \cdot \frac{NB_y + i\,MB_x}{z - i\lambda}
\end{aligned}
\qquad (4.9)
$$

These functions represent a mirror image dislocation with the x and y components of the Burgers vector multiplied by magnification factors M and N respectively. The solution of the problem will then consist of expressions for M and N as functions of $\lambda$ and $\epsilon$, these quantities being determined in such a way that the conditions at the free boundary are satisfied.

Before attempting to find a specific solution, certain additional simplifications will be made. First, the dislocation will be taken as oriented so that its Burgers vector is normal to the boundary, so that $B_x = 0$. This means that only $N(\lambda, \epsilon)$ must be found. Second, the surface layer will be assumed to be thin enough so that it will be sufficient to retain only the first term of each of the series (4.6) and (4.7). Finally, we will weaken the boundary condition (3.24) as in the preceding problem by discarding its imaginary part; in physical terms, this means that the condition on the shear stress will be ignored. The first two of these simplifications are made solely for the purpose of reducing the algebraic

difficulties involved in finding a solution. The final one is of a different character; as in the former problem, it is highly improbable that a practical solution could be found without making it.

On substitution of the stress functions into the boundary condition equation (3.24), the following algebraic expression is obtained:

$$\frac{K_1}{K_1-1}\left[2x^2(-1+N) + 6\lambda^2(-1+N)\right] - (x^2+\lambda^2)(1-N) =$$

$$(-x^2+\lambda^2-6\lambda_1^2)\left(1+\frac{4\lambda h}{x^2+\lambda^2}\right) + \qquad (4.10)$$

$$N(x^2-\lambda^2+6\lambda_2^2)\left(1-\frac{4\lambda h}{x^2+\lambda^2}\right)$$

Here $\lambda_1 = \lambda - h$ and $\lambda_2 = \lambda + h$.

To obtain a reasonable form for the solution, we will only attempt to satisfy (4.10) in the region $|x| << \lambda$, that is, near the intersection of the slip plane with the boundary. This is clearly the region of greatest importance. The explicit solution obtained in this range is

$$N = \frac{\frac{3K_1}{K_1-1} - 16\frac{h}{\lambda} - 2}{\frac{3K_1}{K_1-1} + 4\frac{h}{\lambda} - 2} \qquad (4.11)$$

This may be rewritten as:

$$N = \frac{3 + (1 - 16\frac{h}{\lambda})2\epsilon}{3 + (1 + 8\frac{h}{\lambda})2\epsilon} \qquad (4.12)$$

As a check on this solution, one may note that in the case $\epsilon = 0$ it yields $N = 1$. Thus the previously obtained approximate solution to the homogeneous half plane problem is included in the present solution as a special case. Of particular interest is the fact that in this case the solution is exact in the sense that it satisfies the weakened boundary conditions for all values of x, and not only for $|x| << \lambda$.

It is readily apparent that in general (4.10) would be satisfied for all x only if N were a function of x as well as the other parameters. Since such a form for N is not allowable in our model, we are restricted to an approximate solution which can be made to fit in the region of greatest interest. This limitation is a result of using a single image rather than a series of images; the reduction in algebra and the useful form of the result obtained by the present method, however, more than made up for its approximate nature. The factor N may be regarded as representing the perturbing effect on the homogeneous solution of the introduction of the inhomogeneity. It is not difficult to see then why the present result should be exact for all x in the case $\epsilon = 0$. In general the smaller the value of $\epsilon$, the larger the range of x values over which this solution will closely approach the exact solution.

As a final comment on the result, it should be noted that when the dislocation core approaches the interface between the surface layer and the substrate, interactions may occur which will depend primarily on the microscopic structure of the two media. These interactions clearly can not be predicted by the present continuum theory. Thus the validity of the approach employed here becomes doubtful in the region $\lambda - h < 10\,|\bar{b}|$.

In the following section, some of the implications of equation (4.12) with respect to the behavior of dislocations in real materials will be explored. These implications are of particular interest with regard to the experimental results and their qualitative interpretation discussed in Chapter 1.

## 4.2 Applications

Using equation (4.12) values of the magnification factor N can be computed for particular values of the dimensionless quantities $\frac{E_1}{E_0}$, the

ratio of the Young's moduli in $R_1$ and $R_0$, and $\frac{\lambda}{h}$, the ratio of dislocation distance from the free boundary to the film thickness. The results of some of these calculations are shown in Figure 5 in the form of a family of curves of N vs. $\frac{\lambda}{h}$ for various values of $\frac{E_1}{E_0}$.

The most important feature of these curves is that for $\frac{E_1}{E_0}$ above a certain value all of the curves cross the $\frac{\lambda}{h}$ axis at some value $\frac{\lambda_0}{h}$, where $\frac{\lambda_0}{h} > 1$. At these crossing points N is equal to zero; physically this means that the dislocation is in equilibrium at $\lambda = \lambda_0$. The theory thus predicts that the equilibrium positions for edge dislocations suggested in Chapter 1 can exist in the presence of surface layers with certain properties.

In Figure 6 the dimensionless equilibrium distances $\frac{\lambda_0}{h}$ are plotted as a function of $\frac{E_1}{E_0}$. This curve shows that as one might intuitively expect the equilibrium distances increase as $\frac{E_1}{E_0}$ increases. The slope of the curve decreases monotonically, and it can be shown that $\frac{\lambda_0}{h}$ approaches the limiting value 16 for very large values of $\frac{E_1}{E_0}$.

From Figure 6 the minimum value of $\frac{E_1}{E_0}$ for which an equilibrium position exists can also be determined. This limit, which we will call $(\frac{E_1}{E_0})_c$, corresponds to the value $\frac{\lambda_0}{h} = 1$; that is, it yields an equilibrium position at the interface. As can be seen from the curve, $(\frac{E_1}{E_0})_c \sim 1.3$. This value probably does not have a great deal of real quantitative significance, however, since it is found in a region where the application of continuum methods is of doubtful validity, as mentioned in the preceding section.

Another useful application of equation (4.12) is in the calculation of the force F per unit length acting in the slip direction on edge dislocations as a function of their distance $\ell = \lambda - h$ from the interface between $R_1$ and $R_0$. According to well-known theory discussed by Cottrell (1), this force will have the magnitude $B_y \sigma_{xy}^*(o, -\lambda)$ where $\sigma_{xy}^*(o, -\lambda)$ is the shear stress due to the image dislocation, evaluated at the

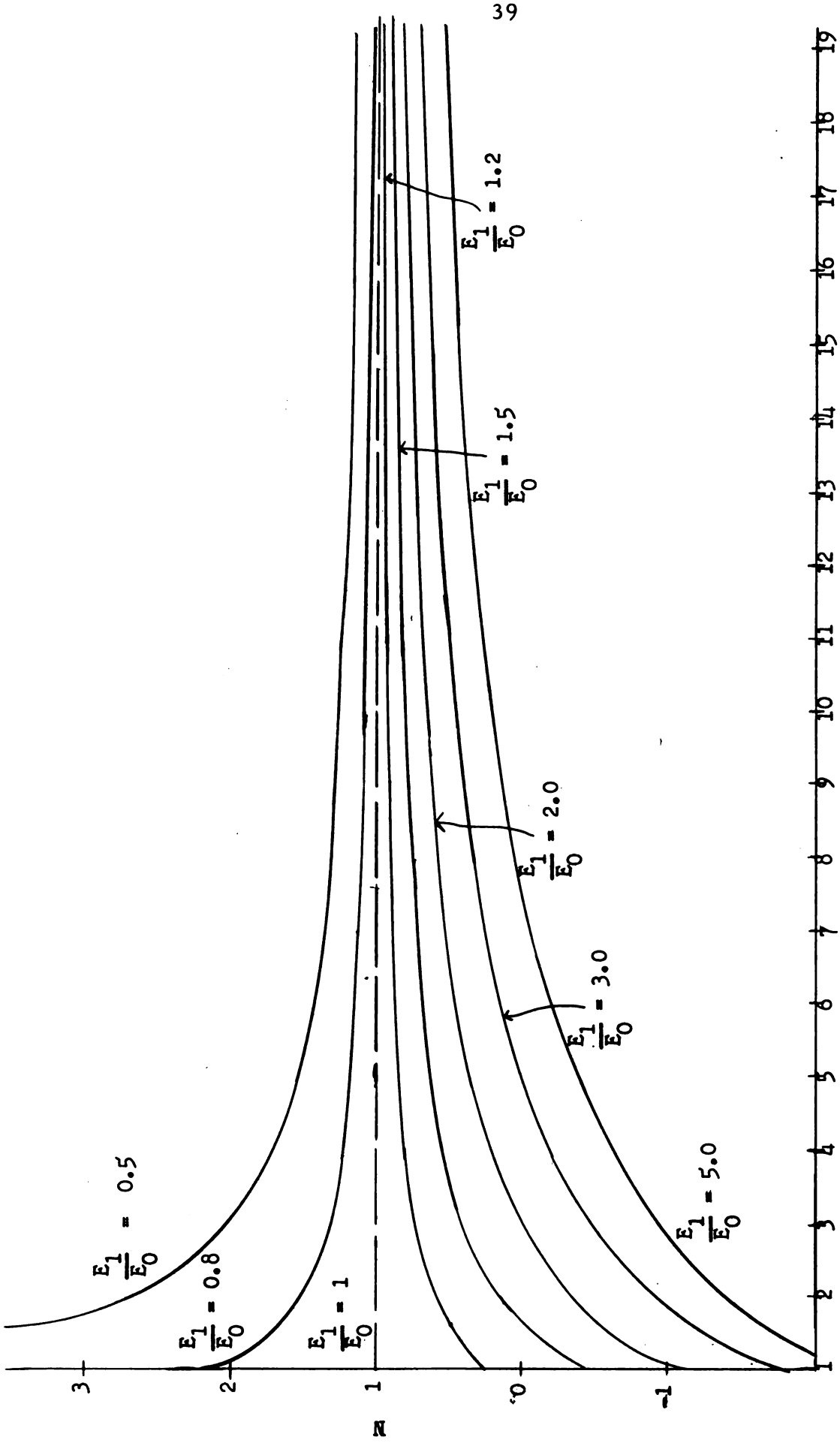


Fig. 5. Magnification factor N vs. dimensionless distance from surface $\frac{\lambda}{h}$ for various ratios of Young's Modulus $\frac{E_1}{E_0}$.

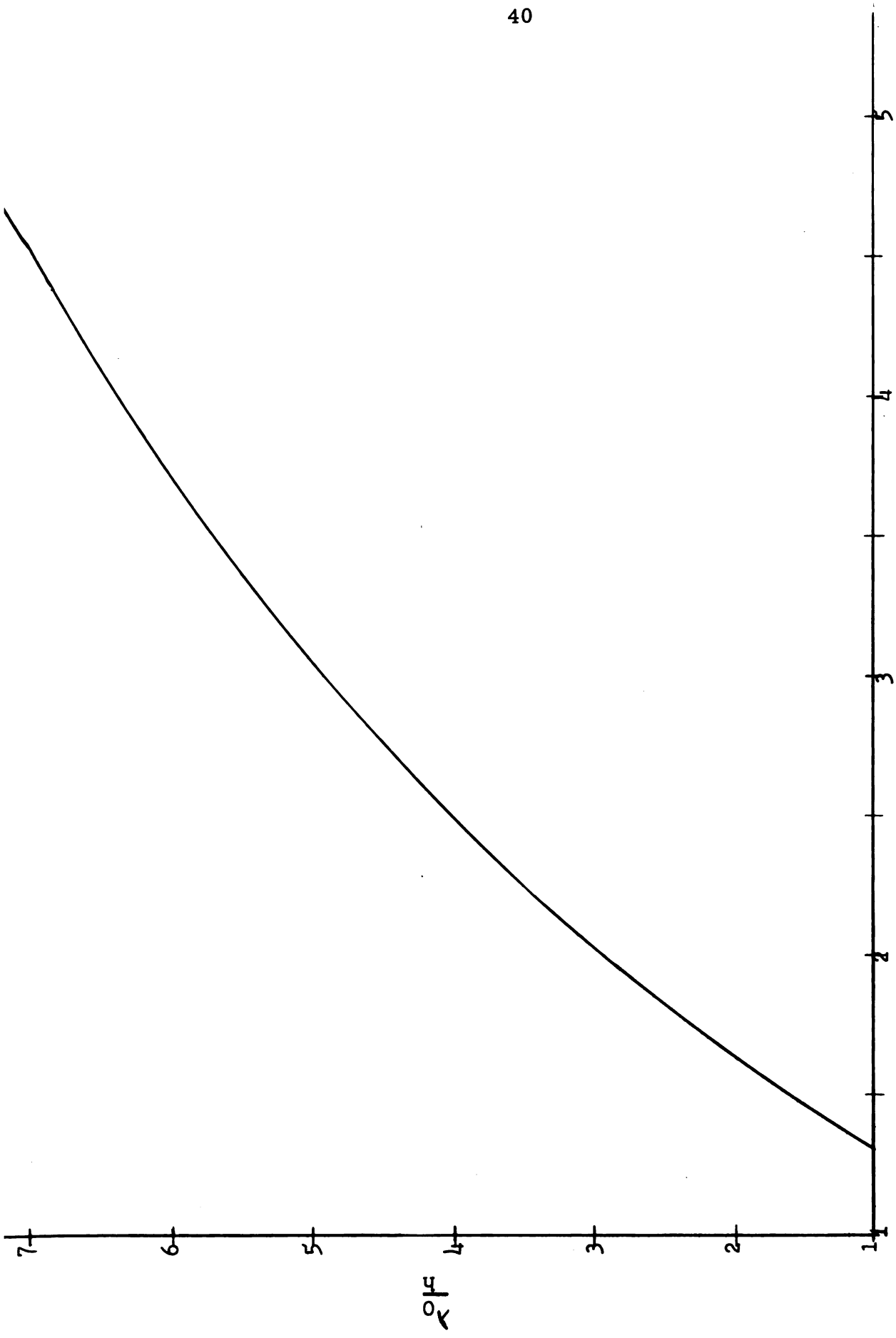


Fig. 6. Dimensionless equilibrium distance from surface $\lambda_0/h$ as a function of the ratio $\frac{E_1}{E_0}$.

location of the real dislocation. In the sign convention to be employed here, positive values of F will represent attraction to the boundary, while negative F indicates repulsion.

Clearly F can be calculated in terms of the parameters h, $B_y$, and $\frac{E_1}{E_0}$ by means of (49), (4.12) and the last of the stress field equations (2.19), in which $B_x$ is taken as zero. It was desired, however, to obtain numerical values for F applicable to actual materials; to do this, numerical values were assigned to the parameters.

For face-centered cubic crystals, which includes all the substrate materials for which calculations were made, the magnitude of the Burgers vector and in this case $B_y$ may be taken as $\frac{a}{2}$ where a is the lattice constant. The values for a used here were given by Kittel (21), and are summarized in Table 3.

Since the materials of interest are not isotropic, it was necessary to use elastic compliances reported for single crystals of each substance to obtain approximate values for the Young's moduli. For this purpose it is reasonable to take $E_0 = \frac{1}{(S_{11})_0}$ and $E_1 = \frac{1}{(S_{11})_1}$, where the $S_{11}$ are the usual elastic compliances as discussed by Huntington (22), and the subscripts $_1$ and $_0$ have their usual significance. The values of $S_{11}$ used in the computations are all as reported by Huntington (22), and are displayed in Table 3.

Table 3. Crystal Properties

| Material | $S_{11}$ | a |
|---|---|---|
| LiF | $1.14 \times 10^{-12} cm^2/dyne$ | 4.02 Å |
| KCl | 2.62 | 6.28 |
| Al | 1.57 | 4.04 |
| Au | 2.33 | --- |
| Cu | 1.50 | --- |
| Gc | 0.978 | --- |
| Ni | 0.734 | --- |
| MgO | 0.408 | --- |

As a final step necessary for making numerical calculations, particular values were assigned to the surface layer thickness h. Figures 7 and 8 show curves of F in dynes/Å x $10^{-7}$ vs. $\ell$ in Å for LiF and KCl substrates having various coatings, with h taken as 50 Å. This value of h is in the range which would be of interest for experimental investigations of surface film effects, and also is small enough so that the assumptions made about film thickness in the theoretical development should be reasonably well satisfied.

Figures 7 and 8 indicate that for certain combinations of materials equilibrium positions corresponding to values F = 0 occur, while for others they do not. It is of particular interest, however, that as the equilibrium positions become farther removed from the interface the slope of the F vs $\ell$ curves at the equilibrium positions becomes increasingly smaller. Such an effect is also observed when the equilibrium position is removed farther from the interface not by increasing E, but by increasing h. This is shown in Figure 9, where plots of F vs for various thicknesses of MgO on LiF are presented.

As a final application of the theory, plots of F vs $\ell$ for aluminum with an aluminum oxide coating are shown in Figure 10, the values $\frac{E_1}{E_0} = 3$ and $\frac{E_1}{E_0} = 4$ being selected. These values of $\frac{E_1}{E_0}$ are suggested by Head (11) as reasonable limits for the two substances. The thickness is taken as 25 Å, a figure in the range reported on the basis of experimental findings by Cabrera and Mott (23), and others. Figure 10 indicates that an equilibrium position may be expected at a depth of 100 to 125 Å, or about 4 to 5 times h, below the interface. For a screw dislocation under the same conditions, Head (11) computed an equilibrium distance about equal to h.

This completes our work with applications of the theory. In the concluding chapter, certain features of the problem will be discussed more fully and some areas in which the results may be extended will be considered.

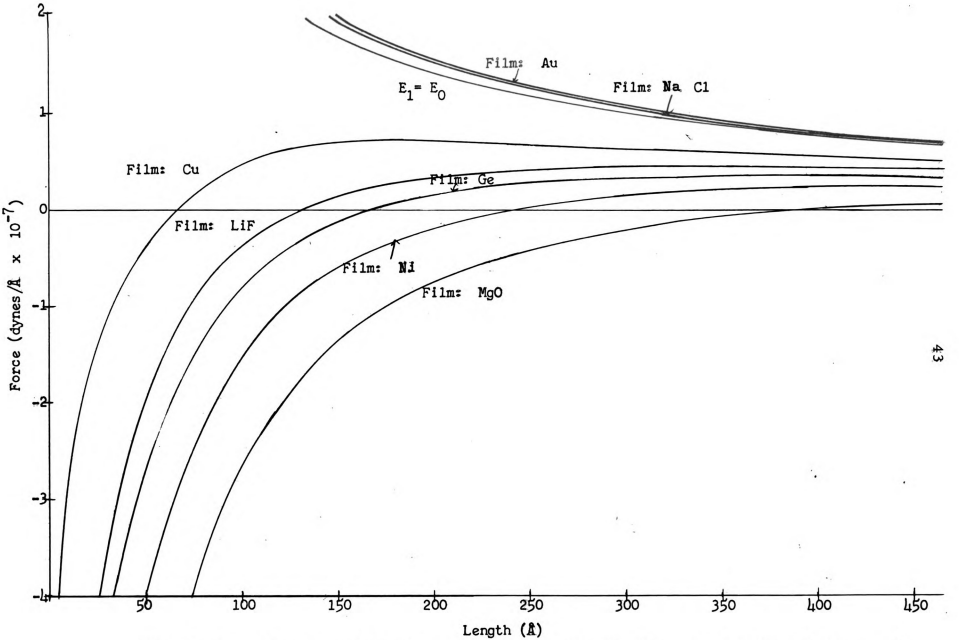




Fig. 7. Force F per unit length on an edge dislocation in KCl as a function of distance $\ell$ from interface for various coatings. All coatings 50 Å in thickness.

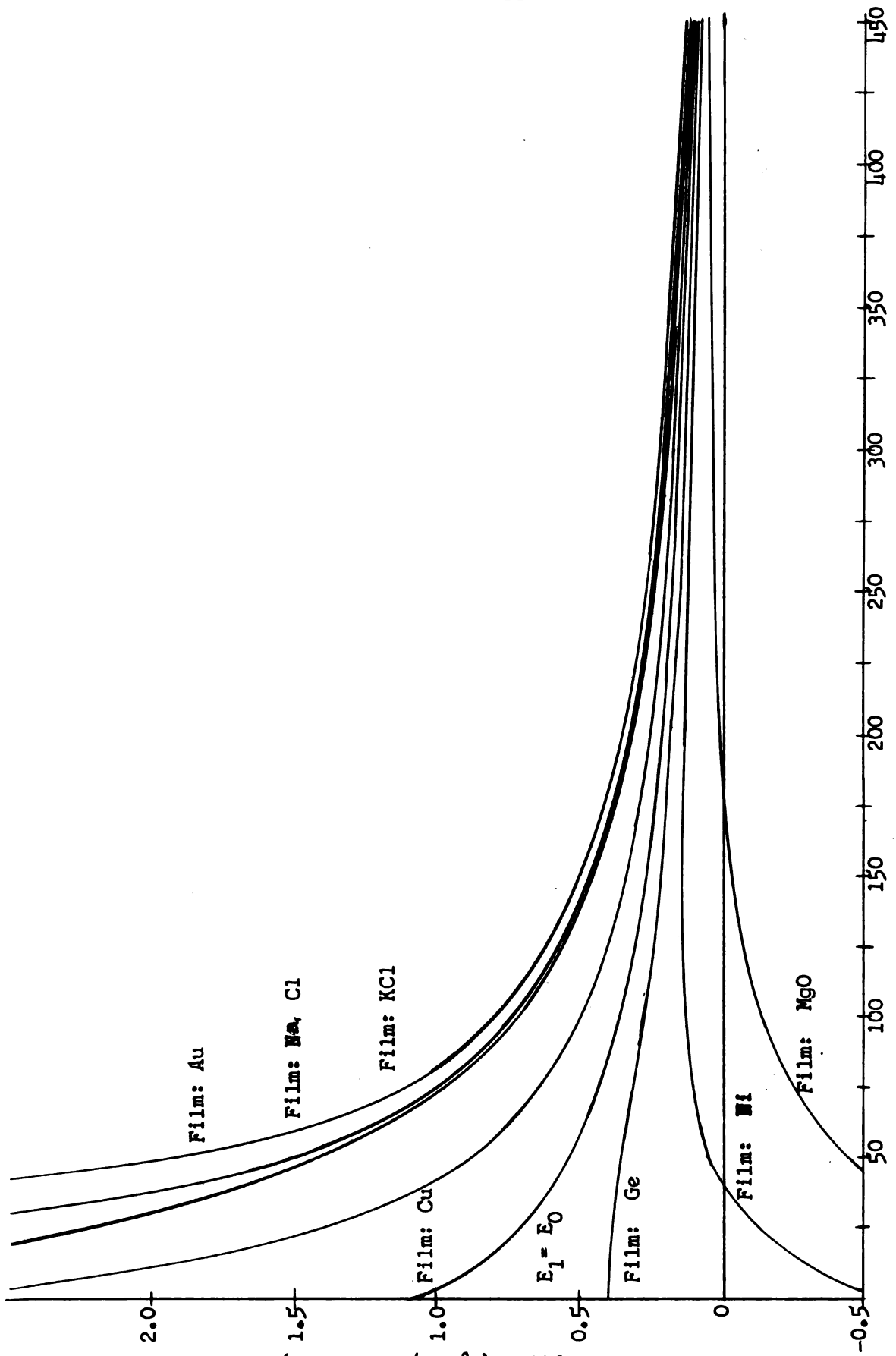


Fig. 8. Force F per unit length on an edge dislocation in LiF as a function of distance $\ell$ from interface for various coatings. All coatings 50Å in thickness.

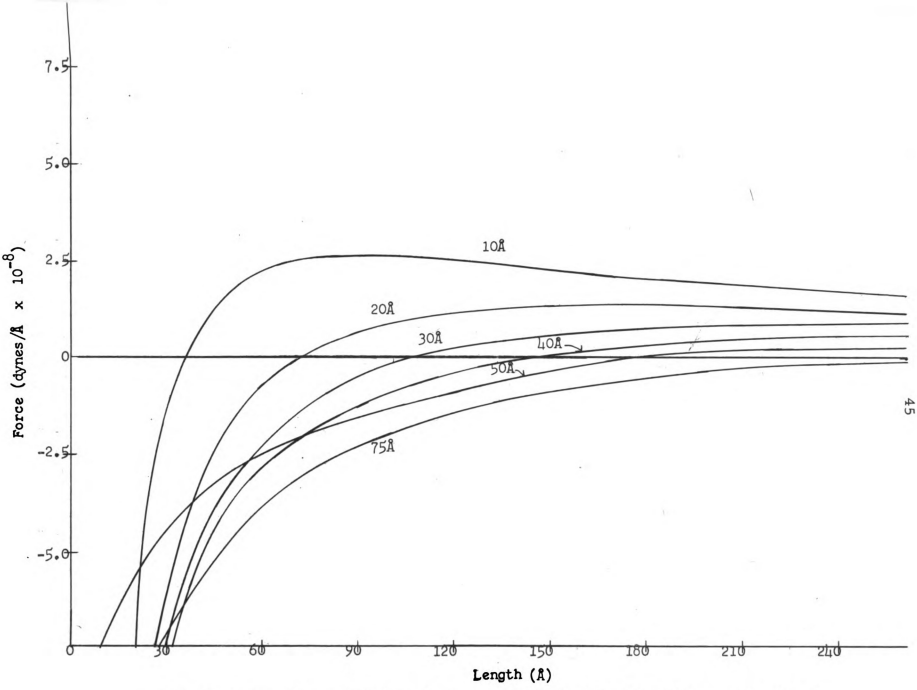




Fig. 9. Force F per unit length on an edge dislocation in LiF as a function of distance $\ell$ from interface, for various thicknesses of MgO coating.

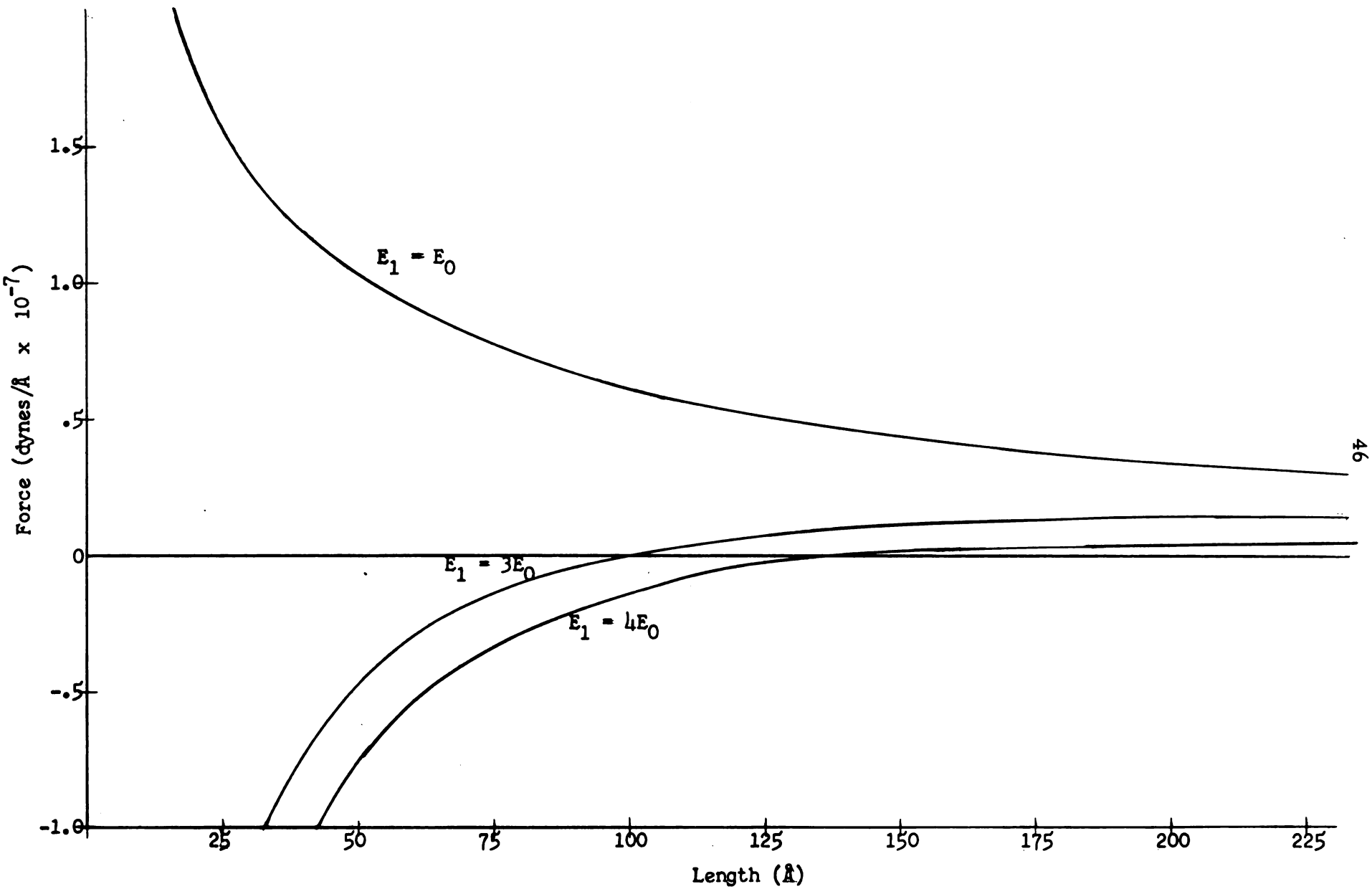




Fig. 10. Force F per unit length on an edge dislocation in Al as a function of distance from interface with aluminum oxide coating. Coating is assumed 25Å in thickness, and two possible ratios of $\frac{E_1}{E_0}$ are used.

# CHAPTER 5

## CONCLUSION

The theory developed in the preceding chapters has led to results which provide a good picture of the behavior of a dislocation near a coated boundary. By treating this situation mathematically as a modification of the case of the homogeneous half plane, these results have been obtained in a simple form which makes them especially useful for applications to particular materials.

The curves shown in Figures 7 through 10 indicate clearly that under certain conditions a surface layer can act as a "barrier to the egress of edge dislocations," in agreement with the suggestion of Westwood (4) discussed in Chapter 1. The approximate value $(\frac{E_1}{E_0})_c \sim 1.3$, obtained from Figure 6, provides a simple criterion for determining under what conditions this barrier effect may be expected to occur. This criterion should be of help in the selection of materials for experiments involving the barrier effect--for example, Roscoe effect investigations.

In addition to indicating the conditions in which a surface layer can act as a barrier, the present results provide useful information about the shape of the potential barrier. As previously noted, the slope of the force-depth curves near the equilibrium position decreases as the equilibrium depth increases. Physically this means that the effective barrier becomes "softer" as the equilibrium depth is increased by increasing either the thickness or Young's modulus of the surface layer. It is apparent that as the barrier becomes softer the amplitude of the displacements from equilibrium produced by thermal agitation, externally

applied forces, or the stress fields of other dislocations, will increase. Consequently the softer the barrier, the smaller will be the probability of finding a dislocation at the calculated equilibrium position.

For small displacements from equilibrium, the force-depth curve is approximately linear so that a dislocation in this region may be regarded as being restrained by a linear spring. The possibility of experimentally looking for acoustic absorption peaks at the resonant frequencies of these oscillator systems therefore suggests itself. Probably such an effect would be small because of the relatively small number of dislocations which would be involved, and would require very carefully controlled conditions in order to be observed.

With regard to extending the present theory, it would be of great interest to develop a method for calculating the equilibrium positions of each one of an array of several parallel edge dislocations on the same slip plane. This might be accomplished by a modification of the elegant theory of Eshelby, Frank and Nabarro (24) in which the first dislocation in an array is considered as being held against a perfectly steep barrier. The effect of barrier softness should be to produce a more even spacing of the equilibrium positions than in the case treated by Eshelby et al.(24). This problem is of particular importance since its solution has the possibility of being checked experimentally. The locations of dislocations in arrays piled up against boundaries have in fact already been determined by etch pit methods by several investigators; the very recent work of Mendelson (25) with NaCl crystals having ozonized surfaces is a good example.

The results obtained here could also be extended by carrying out explicitly the solution for the case $B_x \neq 0$, in which case an expression for the magnification factor M as a function of $\lambda$ and $\epsilon$ would also be required, and by investigating the effect on the solution of retaining some additional terms in the series expansions (4.6) and (4.7). These considerations could be of importance in applications of the theory to the

interpretation of particular experimental results. As examples, it might be of interest to investigate the effect of crystal orientation on the spacing of dislocations in piled up arrays, or to investigate the film thickness dependence of the Roscoe and related effects up to thicknesses where higher order terms in (4.6) and (4.7) would clearly not be negligible.

As another consideration, it may be noted that certain other boundary value problems of interest related to those studied here might advantageously be investigated by similar methods. The problem of a dislocation in a thin film with plane boundaries is one of these. Another, more closely related to the present problem, is that of the substrate with a freely sliding film. As indicated earlier, an approximation to this situation may occur after some critical point is reached in the deformation of real materials. This problem will perhaps be more satisfactory mathematically, in that the conditions at the interface will be sufficiently weak to begin with not to need further weakening since only one displacement component must be continuous across the interface.

## BIBLIOGRAPHY


(1) Cottrell, A. H.
"Dislocations and Plastic Flow in Crystals,"
Clarendon Press, Oxford (1953).

(2) Roscoe, R.
Phil. Mag., 21, 399 (1936).

(3) Andrade, E. N. da C. and Henderson, C.
Phil. Trans. Roy. Soc. A, 244, 177 (1951).

(4) Westwood, A. R. C.
Phil. Mag., 8th Ser., 5, 981 (1960).

(5) Mukai, M.
J. Sci. Hiroshima Univ. A, 22, No. 2, 99 (1958).

(6) Menter, J. W. and Hall, E. O.
Nature, 165, 611 (1950).

(7) Evans, T. and Schwarzenberger, D. R.
Phil. Mag. 8th Ser., 4, 889 (1959).

(8) Schofield, B. H.
"Acoustic Emission Under Applied Stress,"
Lessels and Associates report (August 31, 1961).

(9) Tatro, C.
"Sonic Techniques in the Detection of Crystal Slip in Metals,"
Progress report, Div. of Eng. Res., Mich. State Univ.
(Jan. 1, 1959).

(10) Tatro, C. and Liptai, R.
Unpublished experimental results.

(11) Head, A. K.
Phil. Mag., 44, 92 (1953).

(12) Muskhelishvili, N. I.
"Some Basic Problems of the Mathematical Theory of Elasticity," Noordhoff, Groningen, Holland (1953).

(13) Timoshenko, S. and Goodies, J. N.
"Theory of Elasticity," McGraw-Hill, New York, 2nd ed. (1951).

(14) Love, A. E. H.
"A Treatise on the Mathematical Theory of Elasticity," 4th ed., Dover, New York (1944).

(15) Burgers, J. M.
Proc. Kon. Ned. Akad. Wet., 42, 293 (1939).

(16) Eshelby, J. D.
Phil. Mag., 40, 903 (1949).

(17) Koehler, J. S.
Phys. Rev., 60, 397 (1941).

(18) Churchill, R. V.
"Introduction to Complex Variables and Applications," McGraw-Hill, New York (1948).

(19) Morse, P. M. and Feshbach, H.
"Methods of Theoretical Physics, Part I," McGraw-Hill, New York (1953).

(20) Read, W. T.
"Dislocations in Crystals," McGraw-Hill, New York (1953).

(21) Kittel, C.
Introduction to Solid State Physics, 2nd ed., Wiley, New York (1961).

(22) Huntington, H. B.
"Solid State Physics," vol. 7, Seity and Turnbull eds., Academic Press, New York (1958).

(23) Cabrero, N. and Mott, N. F.
Rep. Prog. Phys., 12, 163 (1948-49).

(24) Eshelby, J. D., Frank, F. C. and Nabarro, F. R. N.
Phil. Mag., 42, 351 (1951).

(25) Mendelson, S.
J. Appl. Phys., 33, 2182 (July, 1962).

# APPENDIX

It is of help in visualizing dislocation stress fields to have plots of the stress components for the important case of a dislocation in an infinite medium. Curves of this type are provided in Figures 11 through 13.

These plots show the dimensionless stresses $\sigma_{xx}^{*} = \frac{\sigma_{xx}}{K}$, $\sigma_{yy}^{*} = \frac{\sigma_{yy}}{K}$, and $\sigma_{xy}^{*} = \frac{\sigma_{xy}}{K}$ as a function of the dimensionless distance $\frac{y}{B_y}$ for a dislocation with Burgers vector $\vec{b} = B_y \hat{j}$. Plots are given for various positive values of the dimensionless distance $\frac{x}{B_y}$; since $\sigma_{xx}^{*}$ and $\sigma_{xy}^{*}$ are odd functions of x while $\sigma_{xy}^{*}$ is an even function of x, the form of the curves for negative values of $\frac{x}{B_y}$ is apparent.

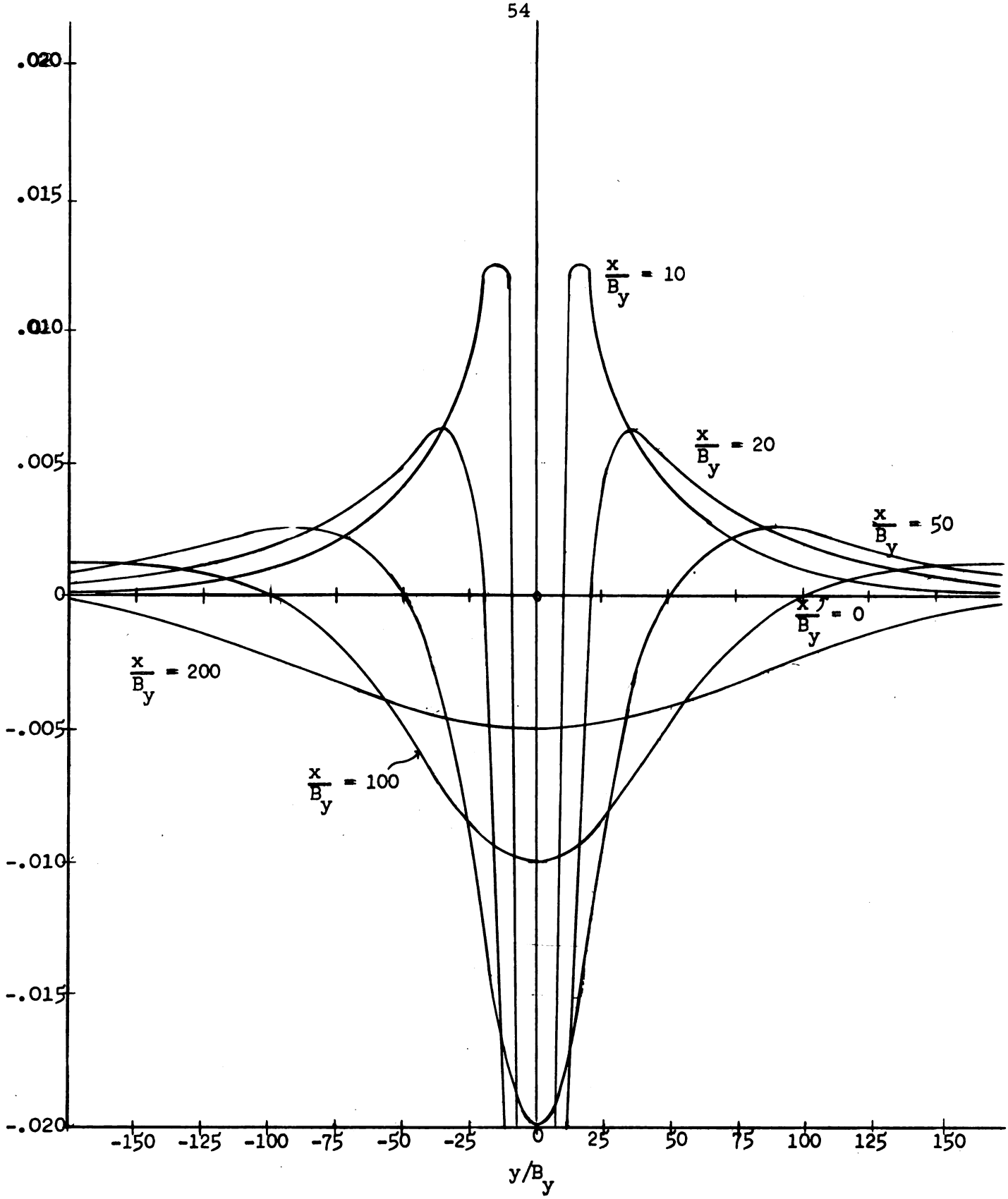


Fig. 11. Dimensionless stress $\sigma_{xx}^{*}$ for an edge dislocation with Burgers vector $B_y\hat{j}$, as a function of $\frac{y}{B_y}$ for various values of $\frac{x}{B_y}$.

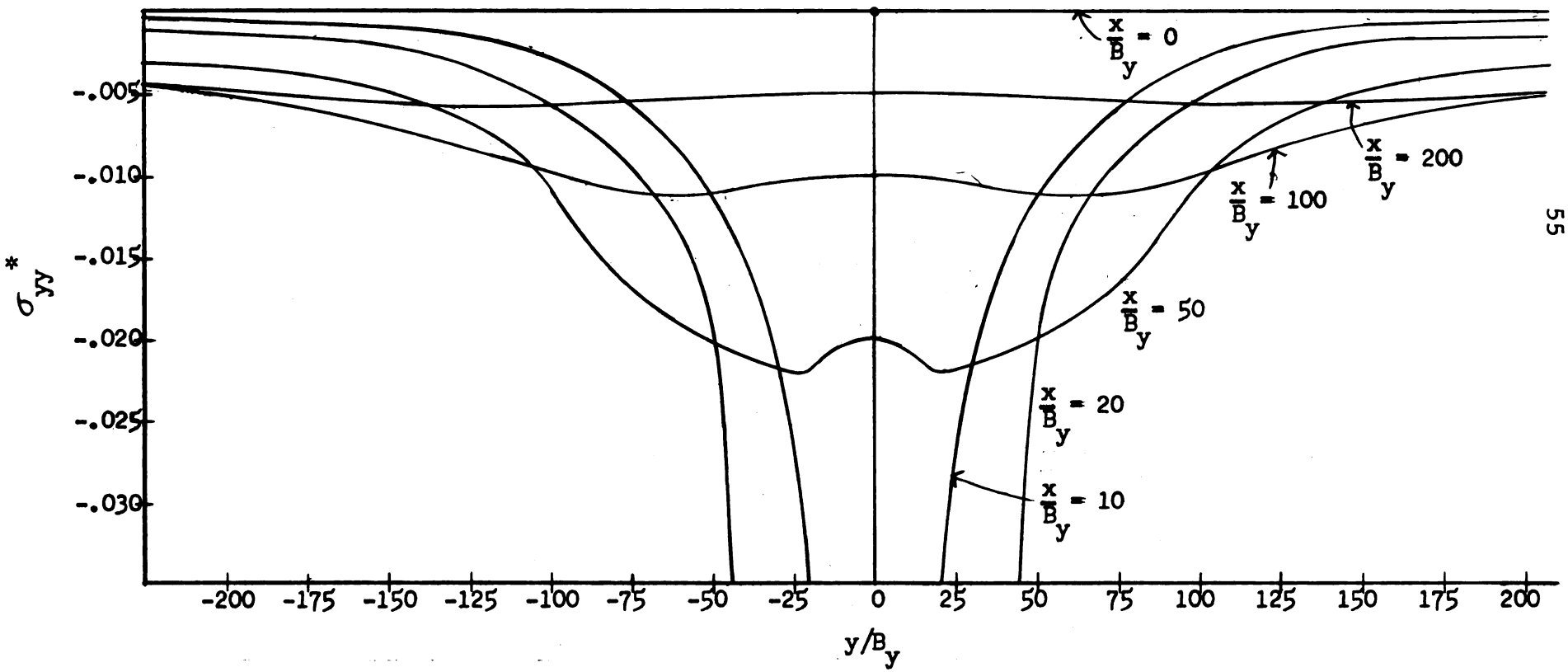


Fig. 12. Dimensionless stress $\sigma_{yy}^*$ for an edge dislocation with Burgers vector $B_y\hat{j}$, as a function of $\frac{y}{B_y}$ for various values of $\frac{x}{B_y}$.

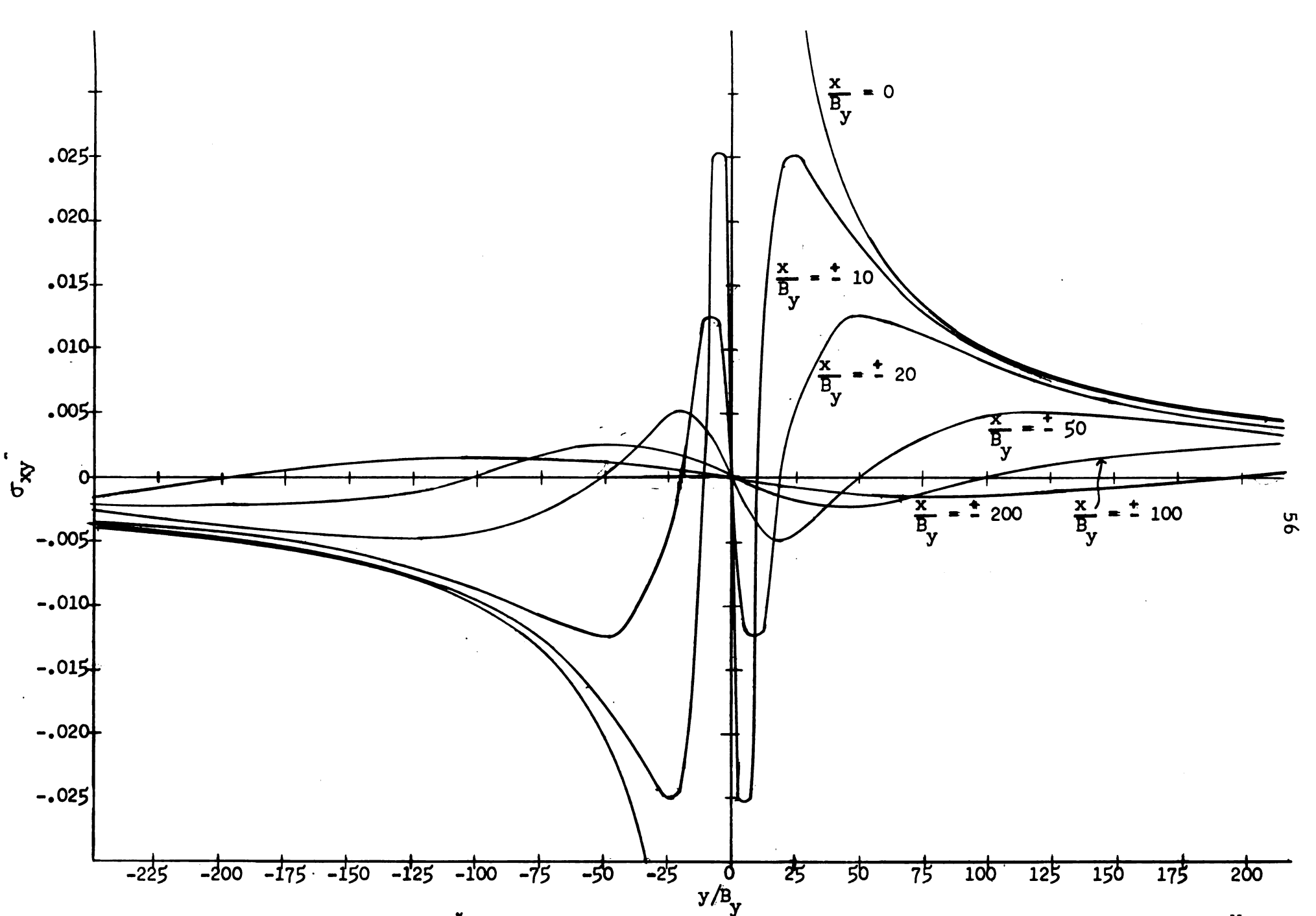


Fig. 13. Dimensionless stress $\sigma_{xy}^{*}$ for an edge dislocation with Burgers vector $B_y\hat{j}$, as a function of $\frac{y}{B_y}$ for various values of $\frac{x}{B_y}$

ROOM USE ONLY